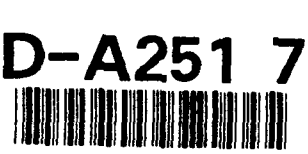

(2)

Office of Naval Research

Grant N00014-90-J-1871

Technical Report No. 7

A CONTINUUM MODEL OF A THERMOELASTIC SOLID CAPABLE OF UNDERGOING PHASE TRANSITIONS

by

Rohan Abeyaratne [1] and James K. Knowles [2]

[1] Department of Mechanical Engineering
Massachusetts Institute of Technology
Cambridge, Massachusetts 02139

[2] Division of Engineering and Applied Science
California Institute of Technology
Pasadena, California 91125

April, 1992

A CONTINUUM MODEL OF A THERMOELASTIC SOLID CAPABLE OF UNDERGOING PHASE TRANSITIONS

by

Rohan Abeyaratne [1] and James K. Knowles [2]

[1]Department of Mechanical Engineering
Massachusetts Institute of Technology
Cambridge, Massachusetts 02139 U.S.A.

[2]Division of Engineering and Applied Science
California Institute of Technology
Pasadena, California 91125 U.S.A.

ABSTRACT

We construct explicitly a Helmholtz free energy, a kinetic relation and a nucleation criterion for a one-dimensional thermoelastic solid capable of undergoing either mechanically- or thermally-induced phase transitions. We study the hysteretic macroscopic response predicted by this model in the case of quasi-static processes involving stress cycling at constant temperature, thermal cycling at constant stress, or a combination of mechanical and thermal loading that gives rise to the shape-memory effect. These predictions are compared qualitatively with experimental results.

1. Introduction. A purely mechanical continuum theory of stress-induced solid-solid phase transitions in tensile bars in stable equilibrium was given by Ericksen (1975) on the basis of the one-dimensional theory of nonlinear elasticity. The principal ingredient of Ericksen's theory is a non-monotonic relation $\sigma = \hat{\sigma}(\gamma)$ between the longitudinal strain γ and the stress σ in the bar: as the strain increases from zero, the stress at first increases to a maximum, then decreases to a minimum and finally increases again. The associated strain-energy per unit mass $\hat{\psi}(\gamma)$ is thus non-convex. If the stress applied to the bar lies between the values associated with the local maximum and the local minimum, the bar may find itself in a configuration in which the stress is constant throughout, as required for equilibrium, but the strain is only *piecewise*

constant, taking any of the three values consistent with the given stress on the three branches of the stress-strain curve. Each branch of the stress-strain curve is associated with a *phase* of the material, the declining branch corresponding to an "unstable phase". A state in which stress is constant but strain suffers jump discontinuities along the bar is viewed as a phase mixture, and the points where the strain jumps are called phase boundaries. Let ρ be the mass per unit reference volume of the bar. At a fixed stress σ that permits phase mixtures, the potential energy per unit reference volume $G(\gamma, \sigma) = \rho \hat{\psi}(\gamma) - \sigma\gamma$ as a function of strain exhibits two minima separated by a maximum. The minima correspond to equilibria in the high- and low-strain phases, while the maximum corresponds to equilibrium in the unstable phase.

A one-parameter family of equilibria of the kind described above in which the parameter is the time t is called a *quasi-static* motion of the bar. Such processes generally involve moving phase boundaries; as a phase boundary sweeps past a particle of the bar, the state of that particle jumps horizontally in the plane of the stress-strain curve from one rising branch to another, or from one potential energy well to another. Phase boundary motion is generally dissipative, even for a thermoelastic material (Knowles, 1979). An energetic notion of *driving traction* f(t) acting on a phase boundary was shown by Abeyaratne and Knowles (1988) to arise naturally in the study of quasi-static processes. If the bar occupies a portion of the x-axis in a reference configuration, and if $x = s(t)$ represents the (Lagrangian) location at time t of a moving phase boundary, then the rate of dissipation of mechanical energy associated with this phase boundary is $f(t)A\dot{s}(t)$, where A is the referential cross-sectional area of the bar. As shown in Abeyaratne and Knowles (1988), the construction of a determinate theory of quasi-static motions of the bar requires the introduction of a *kinetic relation* governing the speed of phase boundaries and hence the rate at which phase transitions proceed, as well as a *nucleation criterion* that signals the onset of such a transition. A natural form for a kinetic relation is $\dot{s} = V(f)$, where V is a function determined by the material; one type of nucleation criterion specifies a critical level f_* of driving traction, also determined by the material. The predictions of the purely mechanical model

developed by Abeyaratne and Knowles (1988) are qualitatively consistent with some experimental observations.

Phase transitions are greatly influenced by temperature, and a purely mechanical theory of the kind described above is incapable of accounting for their thermal aspects. In generalizing to the case of a one-dimensional thermoelastic material capable of undergoing phase transitions, one makes use of the Helmholtz free energy density $\hat{\psi}(\gamma, \theta)$, the kinetic relation $\dot{s} = V(f, \theta)$ and the nucleation criterion $f = f_*(\theta)$, where θ is the absolute temperature. A general discussion of such a theory in three dimensions, accounting for both thermal and inertial effects, shows that the notion of driving traction again arises naturally, but now in connection with the rate of entropy production; see Abeyaratne and Knowles (1990). The purposes of the present paper are to construct explicit examples of $\hat{\psi}$, V and f_*, and to compare the predictions of the associated model of quasi-static macroscopic response with experiments on shape-memory materials, paying special attention to the effects of temperature. Previous studies concerned with the modeling of macroscopic response of shape-memory materials include work based on a statistical model by Müller and Wilmansky (1981) and Achenbach and Müller (1985), and papers by Falk (1980, 1988), in which a special Helmholtz free energy is studied, but kinetics and nucleation are not. Tanaka, Tobushi and Iwanaga (1988) attempt to account for kinetics by imposing a relation of the form $s = F(f, \theta)$, where s is the volume fraction of one of the phases, rather than the more natural kinetic law $\dot{s} = V(f, \theta)$ employed here. Jiang (1988) employs a thermoelastic model along with specified kinetics and nucleation criteria in the context of finite anti-plane shear to predict qualitatively some experimental results of interest in geophysics.

Although we limit our attention here to quasi-static processes, one of the primary motivations for the present model is the possibility that, because of its simplicity, it may prove amenable to an analytical study of *fast* phase transitions that takes thermal effects into account. We hope to carry out such a study, making use of analysis of the kind utilized in our earlier work

on fast stress-induced phase transitions in a purely mechanical context; see Abeyaratne and Knowles (1991ab, 1992ab).

The next section is devoted to the basic one-dimensional thermomechanical framework in which the model will be constructed; we describe the details of mixed-phase equilibrium states in a tensile bar, the associated quasi-static processes and the determination of the macroscopic response. The explicit Helmholtz free energy $\hat{\psi}(\gamma, \theta)$ and the corresponding potential energy function $G(\gamma, \sigma, \theta) = \rho\hat{\psi}(\gamma, \theta) - \sigma\gamma$ are constructed in Section 3. In Section 4 we derive a kinetic relation by using an argument based on thermal activation theory, and we describe the nucleation criterion to be used. The final section contains the detailed predictions of the model for stress-cycling at constant temperture, for thermal cycling at constant stress and for the shape-memory effect. We also compare these results qualitatively with some experimental observations reported by Burkart and Read (1953), Grujicic, Olson and Owen (1985b), Krishnan and Brown (1973), Müller and Xu (1991) and Otsuka and Shimizu (1986).

2. Thermo-mechanical framework. We describe here the continuum thermo-mechanical setting within which we shall apply the detailed constitutive model to be constructed in §§ 3 and 4.

2.1. Equilibrium states. Consider a uniform tensile specimen with length L, cross-sectional area A and mass density ρ in a reference configuration. The specimen is viewed here as a one-dimensional bar that occupies the interval [0, L] of the x-axis in this configuration. When the bar is stretched to an equilibrium state, the displacement is assumed to be continuous and piecewise smooth. The bar is modeled as a thermoelastic solid, with a given Helmholtz free energy function $\hat{\psi}(\gamma, \theta)$ per unit mass; $\theta = \theta(x)$ is the absolute temperature, assumed continuous and piecewise smooth, and $\gamma = \gamma(x)$ is the longitudinal strain, both at the particle whose Lagrangian coordinate is x. We require the strain to satisfy $\gamma > -1$, so that the deformation is

one-to-one. The stress $\sigma(x)$ and specific entropy $\eta(x)$ at a particle are constitutively related to the strain $\gamma(x)$ and the temperature $\theta(x)$ by

$$\sigma = \hat{\sigma}(\gamma, \theta) \equiv \rho \hat{\psi}_{\gamma}(\gamma, \theta), \qquad \eta = \hat{\eta}(\gamma, \theta) \equiv - \hat{\psi}_{\theta}(\gamma, \theta) . \tag{2.1}$$

Suppose that the bar is in mechanical and thermal equilibrium with a given stress applied at each end and in the presence of a heat bath at a given temperature, body forces being absent. Then necessarily $\sigma(x) = \sigma$ = constant, $\theta(x) = \theta$ = constant along the bar, where σ is the applied stress and θ is the temperature of the surroundings. If the stress response function $\hat{\sigma}(\gamma, \theta)$ is monotonically increasing in γ at the given temperature, then $(2.1)_1$ is satisfied at the given stress σ and the given temperature θ for only one value of the strain γ, which therefore is also constant everywhere in the bar. It then follows from $(2.1)_2$ that η has this property as well. Thus in the presence of a monotonic stress-strain relation, homogeneous equilibrium states of stress and temperature give rise to homogeneous states of strain and entropy as well.

On the other hand, suppose that at the temperature θ, the function $\hat{\sigma}(\gamma, \theta)$ at first increases with γ, then decreases and finally increases again, as is the case in what follows; see Figure 1. Then if the given stress σ is in a suitable range, $(2.1)_1$ is satisfied for *three* different values of the strain; two of these are on the rising branches of the stress-strain curve (branches 1 and 3 in the figure), while the third is on the declining branch (branch 2). It is now possible to have distributions of strain and entropy that are only *piecewise* constant along the bar, despite the fact that stress and temperature are everywhere constant. In this event, two particles that bear distinct strains at the same stress and temperature are said to be in different *phases* of the material. The different branches of the stress-strain curve are thus identified with different material phases, and we speak of a low-strain phase, an intermediate "unstable phase", and a high-strain phase corresponding respectively to branches 1, 2 and 3. We shall be concerned in particular with

two-phase equilibrium states at a stress σ and a temperature θ for which $\gamma = \bar{\gamma}$ and $\eta = \bar{\eta}$ for $0 \le x < s$, $\gamma = \overset{+}{\gamma}$ and $\eta = \overset{+}{\eta}$ for $s < x \le L$, *always with* $\bar{\gamma}$ *in the high-strain phase,* $\overset{+}{\gamma}$ *in the low-strain phase.* Since necessarily $\hat{\sigma}(\bar{\gamma}, \theta) = \hat{\sigma}(\overset{+}{\gamma}, \theta) = \sigma$, these strains are related to the stress through

$$\bar{\gamma} = \hat{\gamma}_3(\sigma, \theta), \quad \overset{+}{\gamma} = \hat{\gamma}_1(\sigma, \theta)\,, \tag{2.2}$$

where $\hat{\gamma}_1(\cdot, \theta)$ and $\hat{\gamma}_3(\cdot, \theta)$ are the branch-1 and branch-3 inverses of $\hat{\sigma}(\cdot, \theta)$; see Figure 1. (Numerical subscripts will always refer to the corresponding branch of the stress-strain curve.) The interface $x = s$ at which the strain and entropy jump is a *phase boundary*. The *overall elongation* of the bar in such a two-phase equilibrium state is given by

$$\delta = \bar{\gamma}\, s + \overset{+}{\gamma}\, (L - s) = \hat{\gamma}_3(\sigma, \theta)s + \hat{\gamma}_1(\sigma, \theta)(L-s). \tag{2.3}$$

2.2. Quasi-static processes. We now consider *quasi-static* processes, by which we mean 1-parameter families of equilibrium states of the kind described above, the parameter being the time t. The applied stress and the heat bath temperature are now functions of time: $\sigma = \sigma(t)$, $\theta = \theta(t)$, and in a two-phase quasi-static process, one also has $\overset{\pm}{\gamma} = \overset{\pm}{\gamma}(t)$, $\overset{\pm}{\eta} = \overset{\pm}{\eta}(t)$, $s = s(t)$ and $\delta = \delta(t)$.

Let

$$\hat{\varepsilon}(\gamma, \theta) = \hat{\psi}(\gamma, \theta) + \theta\hat{\eta}(\gamma, \theta) \tag{2.4}$$

be the internal energy of the material, measured per unit mass. For the two-phase quasi-static process, set

$$\overset{\pm}{\varepsilon}(t) = \hat{\varepsilon}(\overset{\pm}{\gamma}(t), \theta(t)), \tag{2.5}$$

so that the total internal energy in the bar at time t is

$$E(t) = \rho A \left[\tilde{\varepsilon}(t)s(t) + \overset{+}{\varepsilon}(t)\,(L-s(t)) \right]. \tag{2.6}$$

If Q(t) is the rate at which heat is supplied to the bar at time t, the first law of thermodynamics requires that

$$\sigma(t)A\dot{\delta}(t) + Q(t) = \dot{E}(t). \tag{2.7}$$

In the present setting, the second law of thermodynamics asserts that

$$\Gamma(t) \equiv \dot{H}(t) - \frac{Q(t)}{\theta(t)} \geq 0, \tag{2.8}$$

where

$$H(t) = \rho A \left[\tilde{\eta}(t)s(t) + \overset{+}{\eta}(t)(L-s(t)) \right] \tag{2.9}$$

is the total entropy in the bar and $\Gamma(t)$ is therefore the rate of entropy production. Eliminating Q(t) between (2.7) and (2.8) and invoking (2.1), (2.3)-(2.6), (2.9) yields the following alternate representation for $\Gamma(t)$:

$$\Gamma(t) = f(t)\, A\, \dot{s}(t)/\theta(t)\,, \tag{2.10}$$

where we have set

$$f(t) = \rho \left\{ \overset{+}{\psi}(t) - \bar{\psi}(t) \right\} - \sigma(t) \left\{ \overset{+}{\gamma}(t) - \bar{\gamma}(t) \right\}, \tag{2.11}$$

and

$$\overset{\pm}{\psi}(t) = \hat{\psi}(\overset{\pm}{\gamma}(t), \theta(t)) \, . \tag{2.12}$$

The inequality (2.8) of the second law may thus be written in the form

$$f(t) \, \dot{s}(t) \geq 0 \, . \tag{2.13}$$

There is an alternative representation for f(t) in terms of the Gibbs free energy per unit reference volume $\hat{g}(\gamma, \theta)$ defined by

$$\hat{g}(\gamma, \theta) = \rho \, \hat{\psi}(\gamma, \theta) - \hat{\sigma}(\gamma, \theta) \, \gamma \, ; \tag{2.14}$$

since $\hat{\sigma}(\overset{+}{\gamma}, \theta) = \hat{\sigma}(\bar{\gamma}, \theta) = \sigma$, one finds from (2.14), (2.11) and (2.12) that

$$f(t) = \overset{+}{g}(t) - \bar{g}(t), \tag{2.15}$$

where

$$\overset{\pm}{g}(t) = \hat{g}(\overset{\pm}{\gamma}(t), \theta(t)). \tag{2.16}$$

Thus f coincides with the jump in the Gibbs free energy density across the phase boundary.

The representation (2.10) for the entropy production rate shows that f may be regarded as the sole agent of entropy production, which, in the present circumstances, occurs only because of a moving phase boundary. A result entirely analogous to (2.10) holds under much more general circumstances, as was shown in Abeyaratne and Knowles (1990). The analysis in that paper pertains to a motion involving strain discontinuities in an *arbitrary* continuum in three dimensions, and it accounts both for inertial and thermal effects; it shows that the entropy production rate Γ is composed of three parts: $\Gamma = \Gamma_{loc} + \Gamma_{con} + \Gamma_{s}$. The first, Γ_{loc}, arises from internal dissipation in the bulk material of the continuum, vanishing if the material is thermoelastic; the second, Γ_{con}, arises from heat conduction, vanishing in the presence of uniform temperature fields. The third contribution, Γ_{s}, arises from moving surfaces of strain discontinuity. The representation for Γ_{s} is strictly analogous to (2.10) and involves a single local, scalar "agent of dissipation" f ; in quasi-static processes, this f relates to the jump in the Gibbs free energy across the moving surface precisely as in (2.15). We call f the "driving traction" for two reasons: first, as shown in Abeyaratne and Knowles (1990), for slow *isothermal* processes in an arbitrary continuum, f may be interpreted energetically as a mechanical "traction" - or force per unit area - acting pointwise on the moving surface of strain discontinuity. Secondly, the jump in the Gibbs free energy in a phase transition is often referred to by materials scientists as the "driving force" associated with the transition. In the present one-dimensional context, we shall speak of fA as the *driving force*, f as the *driving traction*.

If the driving traction vanishes at each instant, the quasi-static process is said to take place "reversibly", since (2.13) then permits $\dot{s}$ to have either sign, so that the phase boundary may move in either direction, and consequently the transition may proceed either from the low-strain phase to the high strain phase, or *vice versa*. Otherwise, (2.13) and the sign of f fix the sign of $\dot{s}$, and hence the sense of the phase transition: if $f > 0$, a particle jumps *from* the low-strain phase *to* the high-strain phase upon passage of the phase boundary; if $f < 0$, the reverse is true.

We may use the first law (2.7), together with (2.1), (2.3)-(2.6), (2.11), (2.12), to obtain the following representation for Q(t):

$$Q(t) = \rho A\theta(t)\left\{\frac{d\bar{\eta}(t)}{dt}\, s(t) + \frac{d\overset{+}{\eta}(t)}{dt}\,(L-s(t))\right\} - \left\{\frac{f(t)}{\rho} + \lambda(t)\right\}\rho A\dot{s}(t), \tag{2.17}$$

where

$$\lambda(t) = \theta(t)\{\overset{+}{\eta}(t) - \bar{\eta}(t)\} \tag{2.18}$$

is the latent heat associated with the transition. The contents of the second brace in (2.17) represent the heat given off by the bar when a unit mass of material crosses the phase boundary. If the transition takes place reversibly, so that $f(t) = 0$, this heat coincides with the latent heat.

In what follows, we shall also need to consider *single*-phase quasi-static processes in which the equilibrium state at each instant is such that the strain and the entropy are uniform throughout the bar, and the strain belongs to the same branch of the stress-strain curve throughout the process. For processes of this kind, the thermoelastic nature of the material implies that the entropy production rate $\Gamma(t)$ vanishes at every time t, so the second law (2.8) is automatically satisfied.

2.3. Macroscopic response. In the thermomechanical loading processes of interest here, the histories of the thermal variable $\theta(t)$ and one of the two mechanical variables $\sigma(t)$ and $\delta(t)$ are to be prescribed, and the resulting history of the remaining mechanical variable is to be determined. In an isothermal constant-elongation-rate mechanical loading process, for example, one would specify $\theta(t)$ and $\dot{\delta}(t)$ to be given constants during the process, with $\sigma(t)$ to be found. In thermal loading, one might prescribe constant values for $\sigma(t)$ and $\dot{\theta}(t)$, with $\delta(t)$ to be determined. When the quasi-static process generated by such a program of loading involves two phases, one

first makes use of (2.2) to express $\bar{\gamma}(t)$ and $\overset{+}{\gamma}(t)$ in terms of $\sigma(t)$ and $\theta(t)$; substituting these expressions into (2.3) yields a single equation relating $\delta(t)$, $\sigma(t)$, $\theta(t)$ and $s(t)$:

$$\delta(t) = \hat{\gamma}_3(\sigma(t), \theta(t))\, s(t) + \hat{\gamma}_1(\sigma(t), \theta(t))\, (L\text{-}s(t)). \tag{2.19}$$

Since in any program of loading only two of the four functions of time entering (2.19) are known, further information must be supplied to yield an additional equation and hence a determinate theory. Requiring the process to take place reversibly, for example, would provide the additional equation $f = 0$. More generally, such supplementary information is provided by the *kinetic relation* controlling the evolution of the phase transition. We take this to be a relation which gives $\dot{s}(t)$ (a measure of the rate at which the transition proceeds) in terms of the driving traction $f(t)$ and the temperature $\theta(t)$; such a relation can be written in the form:

$$\dot{s}(t) = V(f(t), \theta(t)), \tag{2.20}$$

where V is a given function determined by the material. Because of the entropy inequality (2.13), the function V must satisfy

$$V(f, \theta)f \geq 0 \tag{2.21}$$

for all permissible values of f and θ. With the help of (2.2), (2.12) and (2.11), one can express $f(t)$ in terms of $\sigma(t)$ and $\theta(t)$, so that (2.20) may equally well be written in the form

$$\dot{s}(t) = v(\sigma(t), \theta(t)), \tag{2.22}$$

where v is a constitutively determined function related to V. Some discussion motivating the form (2.20) for the kinetic relation may be found in Abeyaratne and Knowles (1990, 1992b).

For a loading process in which $\delta(t)$ and $\theta(t)$ are known, (2.19) and (2.22) comprise two equations for $s(t)$ and $\sigma(t)$; if $\sigma(t)$ and $\theta(t)$ are known, (2.19) and (2.22) are to be used to find $s(t)$ and $\delta(t)$.

We shall encounter quasi-static processes in which the entire bar is in a single phase for an initial interval of time and in two-phase states for subsequent times. The instant of time and the point in the bar at which the transition from the single-phase to the two-phase configuration is initiated are determined by a *nucleation criterion*. Suppose first that, until a certain instant, the bar is in a uniform low-strain configuration. As in our purely mechanical model (Abeyaratne and Knowles 1988, 1991ab, 1992ab), we assume that the transition to the mixed-phase configuration occurs at $x = 0$ when the driving traction f at the incipient phase boundary would be at least as great as a certain materially-determined critical value: $f \geq f_{13}(\theta)$. The particle at $x = 0$ then jumps from branch 1 of the stress-strain curve, or the low-strain phase, to branch 3, or the high-strain phase, causing a phase boundary to enter the bar and then move in accordance with the kinetic relation. Since the velocity of the phase boundary must be positive shortly after nucleation, the entropy inequality (2.13) requires $f_{13} \geq 0$. Suppose that the phase boundary continues to move until it reaches $x = L$, at which time the bar is entirely in the high-strain phase. If a quasi-static *unloading* process is now begun, the bar will remain in the single-phase, high-strain state until the stress and temperature are such that f reaches the nucleation value $f_{31}(\theta)$ for the *reverse* transition. When this occurs, the particle at $x = L$ will jump to the low-strain phase, and a phase boundary will enter the bar from this point. The entropy inequality requires that $f_{31} \leq 0$.

In real materials, the location of the nucleation site is presumably strongly influenced by non-homogeneities. Because our bar is uniform, the location of the nucleation site is rather arbitrary. In the case of a bar rendered "non-homogeneous" by means of a slight uniform taper with the small end at $x = 0$, the low-strain-to-high-strain transition would *necessarily* start at $x = 0$, the reverse transition at $x = L$, as we have assumed above; see Abeyaratne and Knowles (1988).

In the next two sections, we construct an explicit Helmholtz free energy function $\hat{\psi}(\gamma, \theta)$, a particular kinetic response function V and a specialized version of the nucleation criterion. The Helmholtz function is of the non-convex type associated with non-monotonic stress-strain relations of the kind represented schematically in Figure 1. The kinetic response function V is modeled on the notion of a "thermally activated" phase transition. When utilized in the framework set out above, the functions $\hat{\psi}$ and V so constructed, together with the nucleation criterion, serve to provide a simple pilot theory whose predictions of quasi-static response can be compared with experiment.

3. Helmholtz free-energy function. In this section we construct explicitly a particular Helmholtz free-energy function $\hat{\psi}$ that is capable of modeling certain features of thermoelastic phase transformations; the final form of $\hat{\psi}$ is displayed in § 3.4. Our intent is to supply a model which, while taking thermal effects into account, preserves the simplicity of the "trilinear" stress-strain relation used in some of our earlier purely mechanical studies of stress-induced phase transitions in solids; see Abeyaratne and Knowles (1991ab, 1992ab). In the latter context, these investigations show that the trilinear model permits, for example, the construction of explicit global solutions of some *dynamic* problems involving fast phase transitions. Since there are major open questions as to when such dynamic problems are well-posed, it is desirable to have - if possible - a simple, analytically amenable model that will provide helpful insights before undertaking computations based on more realistic assumptions. In the present paper, we

develop such a model and apply it to the study of thermal and mechanical *quasi-static* load cycling (Section 5). In the future we hope to study fast phase transitions in the present setting.

3.1. The stress-strain-temperature relation. The starting point in our construction of the Helmholtz free energy function is the relation $\sigma = \hat{\sigma}(\gamma, \theta)$ between stress and strain at fixed temperature, which will be specified piecewise in the γ, θ- plane. Let $\gamma = \gamma_*, \theta = \theta_* > 0$ be the *critical point* in this plane: it is assumed that for $\theta > \theta_*$, the material exists in only a single phase no matter what the stress level, while two phases are available for $\theta < \theta_*$. The stress response function $\hat{\sigma}$ must therefore be a monotonically increasing function of γ for $\theta > \theta_*$. On the other hand, at each temperature $\theta < \theta_*$, as the strain γ increases from -1, we require $\hat{\sigma}$ to increase for $-1 < \gamma < \gamma_M(\theta)$, then decrease over an intermediate range $\gamma_M(\theta) < \gamma < \gamma_m(\theta)$, and finally increase again, as in Figure 1. In order to make this more precise, let $\gamma_M(\theta)$ and $\gamma_m(\theta)$ be linear functions of temperature defined for $0 < \theta \leq \theta_*$ by

$$\gamma_M(\theta) = \gamma_* + M(\theta - \theta_*), \qquad \gamma_m(\theta) = \gamma_* + m(\theta - \theta_*), \qquad 0 < \theta \leq \theta_*, \tag{3.1}$$

where γ_*, M and m are material constants, with $\gamma_* > 0$. We require that $-1 < \gamma_M(\theta) < \gamma_m(\theta)$, so that the constants M and m, though not necessarily positive, must satisfy

$$m < M < (1 + \gamma_*)/\theta_*. \tag{3.2}$$

The quadrant $\gamma > -1, \theta > 0$ of the γ, θ-plane is divided into four regions P, P_1, P_2 and P_3 by the lines $\theta = \theta_*$, $\gamma = \gamma_M(\theta)$ and $\gamma = \gamma_m(\theta)$. These regions are defined by

$$P = \{(\gamma, \theta) | \gamma > -1, \theta \geq \theta_* \}, \tag{3.3}$$

$$P_1 = \{(\gamma, \theta) | -1 < \gamma \leq \gamma_M(\theta), 0 < \theta < \theta_* \}, \quad P_3 = \{(\gamma, \theta) | \gamma \geq \gamma_m(\theta),), 0 < \theta < \theta_* \} \tag{3.4}$$

$$P_2 = \{(\gamma, \theta) | \gamma_M(\theta) < \gamma < \gamma_m(\theta), 0 < \theta < \theta_* \}, \tag{3.5}$$

where $\gamma_M(\theta)$, $\gamma_m(\theta)$ are given by (3.1); P, P_1 and P_3 are shown dotted and hatched in Figure 2. It is now assumed that for each fixed $\theta < \theta_*$, the stress response function $\hat{\sigma}(\gamma, \theta)$ as a function of strain γ increases *linearly* for $-1 < \gamma \leq \gamma_M(\theta)$, decreases linearly for $\gamma_M(\theta) \leq \gamma \leq \gamma_m(\theta)$, and finally increases linearly for $\gamma \geq \gamma_m(\theta)$. Thus at each temperature below θ_*, the stress-strain curve is a "trilinear" special case of the rising-falling-rising curve of Figure 1. We write

$$\hat{\sigma}(\gamma, \theta) = \begin{cases} \mu\gamma - \mu\alpha\,(\theta - \theta_0) & \text{on } P_1, \\ \mu\left(\gamma - \dfrac{\gamma - \gamma_M(\theta)}{\gamma_m(\theta) - \gamma_M(\theta)}\,\gamma_T\right) - \mu\alpha\,(\theta - \theta_0) & \text{on } P_2, \\ \mu\,(\gamma - \gamma_T) - \mu\alpha\,(\theta - \theta_0) & \text{on } P_3, \end{cases} \tag{3.6}$$

where μ, α, θ_0 and γ_T are material constants whose physical meaning will be made clear below; all four are positive, and $\theta_0 < \theta_*$ as well. Since we intend not to consider points in the single-phase region P in what follows, we do not specify $\hat{\sigma}$ on P. Bearing in mind that different material phases are associated with the different branches of the stress strain curve, we may speak of the respective regions P_1 and P_3 as the low-strain phase and high-strain phase regions of the γ, θ-plane; P_2 is the region that supports the intermediate "unstable phase".

In the trilinear case, the salient features of the stress-strain curve at constant θ are shown in Figure 3. The respective local maximum and minimum values of stress are given by

$$\sigma_M(\theta) = \mu\,[\gamma_M(\theta) - \alpha\,(\theta - \theta_0)], \quad \sigma_m(\theta) = \mu\,[\gamma_m(\theta) - \gamma_T - \alpha\,(\theta - \theta_0)], \qquad 0 < \theta \le \theta_* . \tag{3.7}$$

(It should be noted that, although Figure 3 as shown corresponds to a temperature at which the local minimum $\sigma_m(\theta)$ is negative, this need not be the case at all temperatures.) From (3.1), (3.7) and the requirement $\sigma_M(\theta) > \sigma_m(\theta)$, we find that the inequality $\gamma_T > (M - m)(\theta_* - \theta)$ must hold for all θ between 0 and θ_*. In view of (3.2) this will be the case if and only if the constants M, m, γ_T and θ_* satisfy the restriction

$$\gamma_T > (M - m)\,\theta_* . \tag{3.8}$$

Figure 3 also shows that μ is the elastic modulus of both the low- and high-strain phases of the material; the material constant γ_T represents the horizontal distance between branches 1 and 3 of the stress-strain curve and is called the *transformation strain* relative to the low-strain phase. The coefficient of thermal expansion is α in both low and high-strain phases. The meaning of θ_0 will be explained later.

3.2. Construction of $\hat{\psi}$. From $(2.1)_1$, we may write

$$\rho\hat{\psi}(\gamma, \theta) = \int_0^{\gamma} \hat{\sigma}(\gamma', \theta)\, d\gamma' + \rho\varphi(\theta) \qquad \text{for } (\gamma, \theta) \text{ in } P_1 + P_2 + P_3 , \tag{3.9}$$

where $\varphi(\theta)$ is an as yet undetermined function of temperature, assumed to be continuously differentiable for $0 < \theta < \theta_*$. By (3.6), $\hat{\sigma}$ is a continuous function on the strip $P_1 + P_2 + P_3$, so $\hat{\psi}$ as defined by (3.9) will be continuously differentiable there. A direct calculation using (3.6) gives

$$\int_0^{\gamma} \hat{\sigma}(\gamma', \theta)\, d\gamma' = \begin{cases} \frac{\mu}{2}\gamma^2 - \mu\alpha\,\gamma\,(\theta - \theta_0) & \text{on } P_1\,, \\ -\frac{\mu}{2}\,\frac{\{\gamma_T\,[\gamma - \gamma_M(\theta)]^2 - [\gamma_m(\theta) - \gamma_M(\theta)]\,\gamma^2\}}{\gamma_m(\theta) - \gamma_M(\theta)} - \mu\alpha\,\gamma\,(\theta - \theta_0) & \text{on } P_2\,, \\ \frac{\mu}{2}\,\{(\gamma - \gamma_T)^2 + \gamma_T\,[\gamma_m(\theta) + \gamma_M(\theta) - \gamma_T]\} - \mu\alpha\,\gamma\,(\theta - \theta_0) & \text{on } P_3\,. \end{cases} \tag{3.10}$$

For a thermoelastic material, the specific heat at constant strain is given by $c = -\theta\,\hat{\psi}_{\theta\theta}(\gamma, \theta)$. In view of (3.1), the function on the right side of (3.10) is linear in θ on the high- and low-strain regions P_1 and P_3, so by (3.9), the specific heat is the same in the high- and low-strain phases of our material, being given by

$$c = -\,\theta\,\varphi''(\theta). \tag{3.11}$$

We now require that this specific heat be *constant*; this determines φ to within an inessential additive linear function of θ as

$$\varphi(\theta) = -\,c\theta\,\log\,(\theta/\theta_0)\,, \quad 0 < \theta < \theta_*\,, \tag{3.12}$$

where the constant c is the specific heat at constant strain common to the high- and low-strain phases of our material. Using (3.10) and (3.12) in (3.9) provides the Helmholtz free energy in the form

$$\rho\hat{\psi}(\gamma,\theta)=\begin{cases}\dfrac{\mu}{2}\gamma^2-\mu\alpha\,\gamma(\theta-\theta_0)-\rho\,c\,\theta\,\log(\theta/\theta_0) & \text{on } P_1\,,\\[2ex] -\dfrac{\mu}{2}\,\dfrac{\gamma_T[\gamma-\gamma_M(\theta)]^2-[\gamma_m(\theta)-\gamma_M(\theta)]\,\gamma^2}{\gamma_m(\theta)-\gamma_M(\theta)}-\mu\alpha\,\gamma(\theta-\theta_0)-\rho\,c\,\theta\log(\theta/\theta_0) & \text{on } P_2\,,\\[2ex] \dfrac{\mu}{2}\{(\gamma-\gamma_T)^2+\gamma_T[\gamma_m(\theta)+\gamma_M(\theta)-\gamma_T]\}-\mu\alpha\,\gamma(\theta-\theta_0)-\rho\,c\,\theta\log(\theta/\theta_0) & \text{on } P_3\,,\end{cases} \tag{3.13}$$

where $\gamma_M(\theta)$ and $\gamma_m(\theta)$ are given by (3.1).

3.3. Potential energy, driving traction and latent heat. Since stress and temperature are uniform throughout the bar, it will often be convenient to utilize expressions for the quantities of physical interest in terms of σ and θ. Because the relation (3.6) between stress and strain at fixed θ is not globally invertible, such expressions must be obtained separately for each phase. Inverting the restrictions of (3.6) to P_1 and P_3 yields the form of the relations (2.2) appropriate to the present trilinear material:

$$\tilde{\gamma}=\hat{\gamma}_3(\sigma,\theta)\equiv\gamma_T+\frac{\sigma}{\mu}+\alpha\,(\theta-\theta_0)\quad\text{on } S_1,\qquad \overset{+}{\gamma}=\hat{\gamma}_1(\sigma,\theta)\equiv\frac{\sigma}{\mu}+\alpha\,(\theta-\theta_0)\quad\text{on } S_3\,; \tag{3.14}$$

here S_1 and S_3 are the regions in the θ, σ-plane where the low- and high-strain phases exist, respectively; they are defined by

$$\left.\begin{aligned} S_1&=\{\,(\theta,\sigma)\mid\hat{\sigma}(-1,\theta)<\sigma\le\sigma_M(\theta),\,0<\theta<\theta_*\}\,,\\ S_3&=\{\,(\theta,\sigma)\mid\hat{\sigma}_m(\theta)\le\sigma<\infty\,,\,0<\theta<\theta_*\}\,.\end{aligned}\right\} \tag{3.15}$$

The *coexistence region* $S=S_1\cap S_3$ corresponds to the values of θ, σ for which the low- and high-strain phases can coexist. The region S is the union of the two hatched regions in Figure 4: for definiteness, the figure is drawn under the assumption that the material parameters satisfy

certain inequalities. If this is *not* the case, the region would differ from that shown in Figure 4 in some details.

In terms of θ and σ, the Gibbs free energy per unit reference volume for each phase is given by $\hat{g}_k(\sigma, \theta) = \hat{g}(\hat{\gamma}_k(\sigma, \theta), \theta)$ for k = 1,2,3; for the low- and high-strain phases, one finds from (2.14), (3.13) and (3.14) that

$$\left.\begin{aligned} \hat{g}_1(\sigma, \theta) &= -\frac{1}{2\mu}[\sigma + \mu\alpha(\theta - \theta_0)]^2 + \rho\,\varphi(\theta) \quad \text{on } S_1, \\ \hat{g}_3(\sigma, \theta) &= -\frac{1}{2\mu}[\sigma + \mu\alpha(\theta - \theta_0) + \mu\gamma_T]^2 + \frac{\mu\gamma_T}{2}[\gamma_m(\theta) + \gamma_M(\theta)] + \rho\,\varphi(\theta) \quad \text{on } S_3, \end{aligned}\right\} \tag{3.16}$$

where $\varphi(\theta)$ is given by (3.12). Schematic graphs of $\hat{g}_1$, $\hat{g}_2$ and $\hat{g}_3$ as functions of stress σ at a fixed temperature $\theta > \theta_0$ are shown in Figure 5 . The figure shows that the present model behaves in the manner of the "cusp catastrophe" as in, for example, the van der Waals model of the gas-liquid phase transition; see the discussion in Chapters 5 and 6 of Pippard (1985).

When the bar is in a two-phase equilibrium state, the associated driving traction f can be expressed in terms of θ and σ on the coexistence region S with the help of (2.15), (2.16) and (3.16):

$$f = \hat{f}(\sigma, \theta) \equiv \hat{g}_1(\sigma, \theta) - \hat{g}_3(\sigma, \theta) = \gamma_T\left\{\sigma + \mu\alpha(\theta - \theta_0) + \frac{\mu}{2}[\gamma_T - \gamma_M(\theta) - \gamma_m(\theta)]\right\} \quad \text{on S.} \tag{3.17}$$

It is helpful to introduce the *potential energy* $G(\gamma, \sigma, \theta)$ per unit reference volume by

$$G(\gamma, \sigma, \theta) = \rho\,\hat{\psi}(\gamma, \theta) - \sigma\gamma, \qquad \gamma > -1,\ \sigma > \hat{\sigma}(-1, \theta),\ 0 < \theta < \theta_*\,; \tag{3.18}$$

note that although $G(\gamma, \sigma, \theta)$ is *not* the same as the Gibbs free energy per unit volume, from (2.14), it is clear that $G(\gamma, \hat{\sigma}(\gamma, \theta), \theta) = g(\gamma, \theta)$, and hence that $G(\hat{\gamma}_k(\sigma, \theta); \sigma, \theta) = \hat{g}_k(\sigma, \theta)$. Let θ be fixed in $(0, \theta_*)$. As γ varies with σ fixed in the interval $\hat{\sigma}(-1, \theta) < \sigma < \sigma_m(\theta)$, G has a single minimum, and it occurs at a strain $\gamma = \hat{\gamma}_1(\sigma, \theta)$ in the low-strain phase. If σ is fixed at a value greater than $\sigma_M(\theta)$, G as a function of γ again has a single minimum, but now it occurs at a strain $\gamma = \hat{\gamma}_3(\sigma, \theta)$ in the high-strain phase. On the other hand, if $\sigma_m(\theta) \le \sigma \le \sigma_M(\theta)$, then G has *two* local minima at $\gamma = \hat{\gamma}_1(\sigma, \theta)$ and $\gamma = \hat{\gamma}_3(\sigma, \theta)$, and these are separated by a local maximum; schematic graphs of G vs. γ for various values of σ, all at the same θ, are shown in Figure 6. The stress $\sigma_0(\theta)$ that appears in the figure is the stress at which the values of G at its two minima are the same; it is given explicitly in (3.27) below

From (3.18) and (2.1), one finds that, at each local extremum of $G(\cdot\,; \sigma, \theta)$, the quantities σ, γ and θ are related by $\sigma = \hat{\sigma}(\gamma, \theta)$, so that at an actual equilibrium state, the strain at each particle of the bar must be an extremal of $G(\cdot\,; \sigma, \theta)$.

The difference $G(\hat{\gamma}_1(\sigma, \theta); \sigma, \theta) - G(\hat{\gamma}_3(\sigma, \theta); \sigma, \theta)$ of the values of G at its minima clearly coincides precisely with $\hat{g}_1(\sigma, \theta) - \hat{g}_3(\sigma, \theta)$ and hence also with the driving traction $\hat{f}(\sigma, \theta)$ of the two-phase equilibrium state. When the high-strain minimum is less than the low-strain minimum, f is positive, so by the entropy inequality (2.13), the phase boundary moves to the right, creating more high-strain phase particles at the expense of the low-strain phase. Thus the phase corresponding to the lesser minimum of G is preferred. The same is true when f is negative. Thus we shall call a phase *stable* if it corresponds to an *absolute* minimum of G, *metastable* if the associated extremum of G is a local minimum that need not be absolute, and *unstable* if it corresponds to the local maximum of G. If in a two-phase mixture *both* phases are stable, the driving traction vanishes, and one speaks of *phase equilibrium*. It is important to keep

in mind, however, that during a quasi-static two-phase process, one of the phases may be merely metastable; in the case of solids, metastable states may persist for relatively long times.

The values of G at the two local minima will shift with both stress and temperature. We now assume that two-phase states exist when $\sigma = 0$ and $\theta = \theta_0$; the point $(\theta, \sigma) = (\theta_0, 0)$ is thus required to lie in the coexistence region S, so that

$$\sigma_m(\theta_0) < 0 < \sigma_M(\theta_0) \ , \tag{3.19}$$

and the driving traction $\hat{f}$ of (3.17) is defined at the unstressed state with temperature θ_0 . We further assume that *at the temperature* θ_0 *in the stress-free state, both phases are stable, so that the values of* G *at the two minima coincide, and*

$$\hat{f}(0, \theta_0) = 0 \, ; \tag{3.20}$$

θ_0 is then called the *transformation temperature*. It is easily shown from (3.17) and (3.1) that (3.20) imposes the restriction

$$\gamma_* = \frac{\gamma_T}{2} + \frac{M + m}{2} (\theta_* - \theta_0) \, , \tag{3.21}$$

which we assume to hold from here on. Conversely, (3.21), together with (3.1), (3.2), (3.7) and (3.8), imply that (3.19) holds. With (3.21) in force, the driving traction f can be written as

$$f = \hat{f}(\sigma, \theta) = \gamma_T \, \sigma - \frac{\rho \, \lambda_0}{\theta_0} \, (\theta - \theta_0), \tag{3.22}$$

where the material constant λ_0 is given by

$$\lambda_0 = \frac{\mu}{\rho}\,\gamma_T\,\theta_0\left(\frac{M+m}{2} - \alpha\right). \tag{3.23}$$

From $(2.1)_2$, (2.18), (3.13) and (3.14), the latent heat in the present model is found to be

$$\lambda = \lambda_0 \frac{\theta}{\theta_0}, \tag{3.24}$$

where λ_0 is given by (3.23). Thus the parameter λ_0 represents the *latent heat at the transformation temperature* θ_0.

Since $\sigma_m(\theta) \le \sigma \le \sigma_M(\theta)$ in a two-phase state, one finds from (3.22) that the range of f at each θ is given by

$$f_m(\theta) \le f \le f_M(\theta), \tag{3.25}$$

where

$$f_m(\theta) \equiv \gamma_T\,\sigma_m(\theta) - \frac{\rho\,\lambda_0}{\theta_0}(\theta - \theta_0), \qquad f_M(\theta) \equiv \gamma_T\,\sigma_M(\theta) - \frac{\rho\,\lambda_0}{\theta_0}(\theta - \theta_0). \tag{3.26}$$

At a temperature θ, the stress $\sigma_0(\theta)$ at which the driving traction vanishes is found from (3.22) to be given by

$$\sigma_0(\theta) = \frac{\rho \lambda_0}{\gamma_T} \left(\frac{\theta - \theta_0}{\theta_0} \right), \tag{3.27}$$

so that by (3.22), f can be written as

$$f = \hat{f}(\sigma, \theta) = \gamma_T [\sigma - \sigma_0(\theta)]; \tag{3.28}$$

$\sigma_0(\theta)$ is called the *Maxwell stress* at the temperature θ. By the entropy inequality (2.13), the phase boundary moves into the low-strain phase for $\sigma > \sigma_0(\theta)$, into the high-strain phase for $\sigma < \sigma_0(\theta)$, and the bar is in phase equilibrium for $\sigma = \sigma_0(\theta)$. In particular, nucleation of the low-strain to high-strain phase transition can only occur at a stress at least as great as the Maxwell stress; an analogous remark applies to nucleation of the reverse transition.

From the discussion given above, it is clear that the portion S of the θ, σ-plane in which both phases can exist may be divided into regions in which each phase is stable. Referring to Figure 4, we observe that the portion of the coexistence region S that lies *above* the Maxwell line $\sigma = \sigma_0(\theta)$ corresponds to states θ, σ for which the high-strain phase is stable, while below this line, the low-strain phase is stable; *on* the Maxwell line, *both* phases are stable. In particular, at the transformation temperature θ_0, the low-strain phase is stable in compression, the high-strain phase is stable in tension, and in the unstressed state, both phases are stable.

3.4. Summary. Applicability of the model. For future reference, we list here in final form the representations of $\hat{\psi}$, $\hat{\sigma}$ and $\hat{\eta}$ constructed above; we give only the restrictions of these functions to the low- and high-strain regions P_1 and P_3. Making use of (3.1), (3.21) and (3.23), we find from (3.13) that

$$\rho\hat{\psi}(\gamma, \theta) = \begin{cases} \dfrac{\mu}{2}\gamma^2 - \mu\alpha\,\gamma\,(\theta - \theta_0) - \rho c\,\theta \log(\theta/\theta_0) & \text{on } P_1\,, \\ \dfrac{\mu}{2}(\gamma - \gamma_T)^2 - \mu\alpha\,(\gamma - \gamma_T)(\theta - \theta_0) + \dfrac{\rho\lambda_0}{\theta_0}(\theta - \theta_0) - \rho c\,\theta \log(\theta/\theta_0) & \text{on } P_3\,. \end{cases} \tag{3.29}$$

From (3.6), the stress-strain-temperature relation is

$$\hat{\sigma}(\gamma, \theta) = \begin{cases} \mu\,\gamma - \mu\alpha\,(\theta - \theta_0) & \text{on } P_1\,, \\ \mu(\gamma - \gamma_T) - \mu\alpha\,(\theta - \theta_0) & \text{on } P_3\,. \end{cases} \tag{3.30}$$

Using (3.29) in $(2.1)_2$ gives the entropy-strain-temperature relation as

$$\hat{\eta}(\gamma, \theta) = \begin{cases} \dfrac{\mu\alpha}{\rho}\gamma + c\left[1 + \log(\theta/\theta_0)\right] & \text{on } P_1\,, \\ \dfrac{\mu\alpha}{\rho}(\gamma - \gamma_T) - \dfrac{\lambda_0}{\theta_0} + c\left[1 + \log(\theta/\theta_0)\right] & \text{on } P_3\,. \end{cases} \tag{3.31}$$

According to (3.22), (3.28), the driving traction acting on the interface between a high-strain phase on the left and a low-strain phase on the right in a phase mixture is

$$f = \hat{f}(\sigma, \theta) = \gamma_T\sigma - \frac{\rho\lambda_0}{\theta_0}(\theta - \theta_0) = \gamma_T\left[\sigma - \sigma_0(\theta)\right] \quad \text{on S.} \tag{3.32}$$

The material constants are subject to the inequalities (3.2), (3.8) and the restriction (3.21).

We observe that the form of the stress-strain-temperature relation (3.30) in the low- and high-strain phases is linear in $\theta - \theta_0$, so that one might expect the utility of the model to be limited to modest values of the departure of the temperature from the transformation tempera-

ture θ_0. Also, the nature of our model in the neighborhood of the critical point (γ_*, θ_*), near which the plane is divided into wedge-like regions, is fundamentally flawed, in the sense that, although $\hat{\psi}(\gamma, \theta)$ is continuous on the region $-1 < \gamma < \infty$, $0 < \theta \leq \theta_*$, this is *not* true of its gradient, which, though continuous on the strip $P_1 + P_2 + P_3$, fails to be continuous *at* the critical point. This is not the case, for example, with the Helmholtz free energy functions constructed by Falk (1980, 1988) and by Jiang (1988) for martensitic transformations, both of which describe a smooth bifurcation from single-phase to multiple-phase states near the critical point, as does the corresponding function for the van der Waals fluid; see Pippard (1985). Furthermore, the predictions of the present model are likely to be unrealistic near $\theta = 0$. As a result of these limitations, we confine our attention to temperatures in a subinterval of the interval $(0, \theta_*)$ that includes θ_0 but is well removed from both $\theta = \theta_*$ and $\theta = 0$.

In developing the present model, we have had the thermoelastic martensitic transformation in mind as a prototype. In our setting, a transformation of this type is described as follows. Suppose the tensile bar is in the reference configuration at the transformation temperature θ_0, and therefore at zero stress. Assume the material is such that the latent heat λ_0 is positive. If the bar is now heated to a temperature $\theta > \theta_0$, still at zero stress, it follows from (3.32) that $\hat{f}(0, \theta) < 0$, so the low-strain phase is stable. If instead the bar were *cooled* at zero stress to a temperature less than θ_0, the high-strain phase would be the stable one. In keeping with the terminology of materials science, we would then call the low-strain phase *austenite*, the high-strain phase *martensite*. The reverse would be true if $\lambda_0 < 0$. Although in real materials martensite often exists in many forms, our model acknowledges only one.

4. Kinetic relation and nucleation criterion. In the present section, we construct explicit versions of a kinetic relation and a nucleation criterion of the form described in § 2.

4.1. The kinetic relation. The kinetic relation to be constructed here has the form $\dot{s} = V(f, \theta)$ introduced in (2.20). It is based on the classical notion of "thermally activated" phase transitions; for related discussion, see Porter and Easterling (1981) and Weiner (1970). Our presentation is meant to be illustrative and to provide a physically-based example of a kinetic relation of the form (2.20). Indeed, not all phase transitions need be thermally activated, and it may well be that kinetic relations *not* of the form (2.20) may be appropriate in some circumstances; see Grujicic, Olson and Owen (1985a).

The construction depends critically on the potential energy function $G(\gamma; \sigma, \theta)$ defined in (3.18). Consider a two-phase equilibrium state in the bar, with - as always - particles in the segment $0 < x < s$ in the high-strain phase, those in $s < x < L$ in the low-strain phase. In such a state, the stress must be in the range $\sigma_m(\theta) < \sigma < \sigma_M(\theta)$ if the temperature is θ. The two-well potential G then has two minima, and particles immediately adjacent to the phase boundary on the left and the right must be in states that correspond to the high-strain and low-strain minimum, respectively. As the phase boundary moves through the bar, the particle immediately in front of the interface thus "jumps" from one local minimum to the other. The kinetic relation is constructed by viewing this jumping process on an atomic scale: atoms undergo random thermal fluctuations in their positions and velocities, and their energies vary accordingly. In order to jump from one minimum of G to the other, an atom must acquire an energy at least as great as that of the relevant "energy barrier" at the stress σ and the temperature θ: for an atom undergoing a low-strain to high-strain transition by jumping from the minimum on the left (corresponding to branch 1 of the stress-strain curve) to the one on the right (branch 3) in Figure 6, this barrier - call it B_{13} - is proportional to the minimum-to-maximum height $b_{13}(\sigma, \theta)$ shown in the figure. Since the units of G, and therefore of b_{13}, are those of energy per unit volume, we have

$B_{13} = b_{13}(\sigma, \theta)/r$, where the absolute constant r is the number of atoms per unit reference volume. For the reverse transition, the barrier is $B_{31} = b_{31}(\sigma, \theta)/r$. Under suitable assumptions about the statistics of this process, the probability that the energy of a single atom is at least as great as, say, B, is $\exp(- B/k\theta)$, where k is Boltzmann's constant. The average *rate* at which atoms jump from one minimum to the other is taken to be proportional to the probability of exceeding the corresponding energy barrier. The velocity $\dot{s}$ of the phase boundary, being the macroscopic measure of the net rate at which atoms change from the low-strain phase to the high-strain phase, is taken to be the difference of the average rates associated with the two atomic transitions:

$$\dot{s} = v(\sigma, \theta) = R\left\{\exp[- b_{13}(\sigma, \theta)/rk\theta] - \exp [- b_{31}(\sigma, \theta)/rk\theta]\right\}, \tag{4.1}$$

where $R = n/(rA)$, n is the frequency with which atoms attempt to surmount the relevant energy barrier, and A is the referential cross-sectional area of the bar. For simplicity, we have assumed that n is the same for both phase transitions. We also assume that n is independent of temperature; see the discussion in Weiner (1970). Thus R is an absolute constant.

We next calculate the values of the energy barriers for the particular material described in Section 3. From Figure 6 and the fact that $G = G(\hat{\gamma}_i(\sigma, \theta); \sigma, \theta)$, i = 1,2,3, at the extrema, it is clear that

$$\left.\begin{aligned} b_{13}(\sigma, \theta) &= G(\hat{\gamma}_2(\sigma, \theta); \sigma, \theta) - G(\hat{\gamma}_1(\sigma, \theta); \sigma, \theta), \\ b_{31}(\sigma, \theta) &= G(\hat{\gamma}_2(\sigma, \theta); \sigma, \theta) - G(\hat{\gamma}_3(\sigma, \theta); \sigma, \theta). \end{aligned}\right\} \tag{4.2}$$

Using (3.7) and the explicit form of $\hat{\psi}$ given in (3.13) to calculate G from (3.18) leads to

$$\left.\begin{aligned} b_{13}(\sigma, \theta) &= \frac{\gamma_T}{2\, D(\theta)} \left[\sigma - \sigma_M(\theta)\right]^2 , \\ b_{31}(\sigma, \theta) &= \frac{\gamma_T}{2\, D(\theta)} \left[\sigma - \sigma_m(\theta)\right]^2 , \end{aligned}\right\} \tag{4.3}$$

where

$$D(\theta) = \sigma_M(\theta) - \sigma_m(\theta) , \qquad 0 < \theta \le \theta_* . \tag{4.4}$$

Since $\sigma_M(\theta) > \sigma_m(\theta)$, necessarily $D(\theta) > 0$. By making use of (3.7), (3.1), (3.21), (3.23) and (3.27), one can show that $\sigma_0(\theta) = \left[\sigma_M(\theta) + \sigma_m(\theta)\right]/2$. This fact, together with (3.28), allows one to express the b's in (4.3), and hence the kinetic relation (4.1), in terms of driving traction f. The result is

$$\dot{s} = V(f, \theta) \equiv 2R \exp\left[- \frac{f^2 + \gamma_T^2 D^2(\theta)/4}{2\, \gamma_T\, r\, k\, \theta D(\theta)} \right] \sinh \frac{f}{2rk\theta} . \tag{4.5}$$

Clearly, V is odd in f at each θ, and $V(f, \theta) f \ge 0$, as required by the entropy inequality; see (2.21). Moreover, one can show that, at each fixed θ, $V(f, \theta)$ increases monotonically with f in the range (3.25). From (3.22), it then follows that $v(\sigma, \theta)$ increases monotonically with σ for each θ. A plot of the relation (4.5) when recast in terms of appropriate dimensionless variables will be shown later (see Figure 8).

If the driving traction is small, so that quasi-static processes take place in a nearly reversible manner, one might linearize (4.5) with respect to f, obtaining

$$\dot{s} = v(\theta)\, f , \tag{4.6}$$

where $\nu(\theta)$ is given by

$$\nu(\theta) = \frac{R}{rk\theta} \exp\left[- \gamma_T D(\theta)/(8rk\theta) \right] , \quad 0 < \theta \le \theta_* . \tag{4.7}$$

4.2. The nucleation criterion. For simplicity, we now assume that the nucleation levels of driving traction $f_{13} \ge 0$ and $f_{31} \le 0$ are independent of θ and are thus material constants. Then by (3.22), nucleation occurs when stress and temperature are such that

$$\left.\begin{aligned} \gamma_T\sigma - \frac{\rho\lambda_0}{\theta_0}(\theta - \theta_0) \ge f_{13} \quad &\text{(low-strain to high-strain)} , \\ \gamma_T\sigma - \frac{\rho\lambda_0}{\theta_0}(\theta - \theta_0) \le f_{31} \quad &\text{(high-strain to low-strain).} \end{aligned}\right\} \tag{4.8}$$

The nucleation levels of stress as functions of temperature are found from (4.8) to be

$$\sigma_{13}(\theta) = \frac{f_{13}}{\gamma_T} + \frac{\rho\lambda_0}{\gamma_T\theta_0}(\theta - \theta_0) , \qquad \sigma_{31}(\theta) = \frac{f_{31}}{\gamma_T} + \frac{\rho\lambda_0}{\gamma_T\theta_0}(\theta - \theta_0) , \tag{4.9}$$

for the two types of phase transition. On the other hand, the nucleation levels of temperature as functions of stress are given by

$$\theta_{13}(\sigma) = \theta_0\left(1 + \frac{\gamma_T\sigma - f_{13}}{\rho\lambda_0} \right) , \qquad \theta_{31}(\sigma) = \theta_0\left(1 + \frac{\gamma_T\sigma - f_{31}}{\rho\lambda_0} \right) . \tag{4.10}$$

Suppose momentarily that the material is such that $\lambda_0 > 0$, so that the low-strain phase is austenite, the high strain phase martensite. Assume that the bar is in the reference configuration at zero stress and at the transformation temperature θ_0. Upon cooling at zero stress, martensite will nucleate at the temperature $\theta_{13}(0)$, which by $(4.10)_1$ is necessarily less than θ_0; in the materials science literature, $\theta_{13}(0)$ is denoted by M_s and is called the "martensite start temperature". One can similarly identify $\theta_{31}(0)$ with the "austenite start temperature" A_s.

5. Quasi-static processes. Here we use the explicit forms of the Helmholtz free energy of § 3 and the kinetic relation and nucleation criterion of § 4 to study quasi-static thermo-mechanical processes of the kind described in § 2.3. Let us consider a process of this kind in which the bar remains entirely in the low-strain phase until the instant at which the high-strain phase is nucleated at the left end of the bar, thus generating a two-phase process. We take the nucleation instant to be the time $t = 0$, and we wish to study the histories $\sigma(t)$, $\theta(t)$ and $\delta(t)$ of stress, temperature and elongation during the subsequent evolution of the two-phase state. By the nucleation condition $(4.8)_1$, we have the initial condition

$$\theta_0 \gamma_T \sigma(0) - \rho \lambda_0 [\theta(0) - \theta_0] = \theta_0 f_{13} \ . \tag{5.1}$$

As shown in § 2.3, the macroscopic response of the bar is governed by (2.19) and (2.22). For the material described in § 3, (3.14) can be used to specialize (2.19) to

$$\delta = \gamma_T s + \left[\frac{\sigma}{\mu} + \alpha (\theta - \theta_0) \right] L \ ; \tag{5.2}$$

it follows that during a quasi-static process,

$$\frac{\dot{\delta}}{L} = \gamma_T \frac{\dot{s}}{L} + \frac{\dot{\sigma}}{\mu} + \alpha \dot{\theta} . \tag{5.3}$$

We now use the kinetic relation (4.1) with the energy barriers expressed in terms of stress and temperature by means of (4.3). Eliminating $\dot{s}$ between (4.1) and (5.3) leads to the "master equation" relating $\delta(t)$, $\sigma(t)$ and $\theta(t)$ during an arbitrary quasi-static process:

$$\frac{\dot{\delta}}{L} - \frac{\dot{\sigma}}{\mu} - \alpha \dot{\theta} = \frac{\gamma_T}{L} v(\sigma, \theta) , \tag{5.4}$$

where

$$v(\sigma, \theta) = R \left\{ \exp\left[- \frac{\gamma_T}{2rk\theta} \frac{[\sigma - \sigma_M(\theta)]^2}{\sigma_M(\theta) - \sigma_m(\theta)} \right] - \exp\left[- \frac{\gamma_T}{2rk\theta} \frac{[\sigma - \sigma_m(\theta)]^2}{\sigma_M(\theta) - \sigma_m(\theta)} \right] \right\}, \tag{5.5}$$

and $\sigma_M(\theta)$ and $\sigma_m(\theta)$ are given by (3.7), (3.1).

In the remainder of this section, we investigate the detailed predictions of the present model for isothermal stress cycling, for temperature cycling at constant stress, and for a process that illustrates the shape-memory effect. We assume throughout that $\lambda_0 > 0$, so that the low strain phase corresponds to austenite.

5.1. Isothermal mechanical loading and unloading. We first consider an isothermal, grip-controlled quasi-static process in which the elongation rate is prescribed. The specimen is initially unstressed at a temperature θ, which we assume to exceed the stress-free nucleation temperature $\theta_{13}(0)$. By (5.2) with $s = 0$, $\sigma = 0$, the initial elongation δ_0 relative to the reference configuration is $\delta_0 = \alpha (\theta - \theta_0) L$. The bar is then stretched at a constant elongation rate $\dot{\delta} = q$.

the temperature being held constant at the value θ. We wish to determine the resulting relation between the stress σ and the elongation $\Delta = \delta - \delta_0$ relative to the *initial* configuration. During the initial period of loading, the bar remains in the low-strain phase, and this relation is simply $\sigma = \mu\, \Delta/L$. When the stress reaches the critical value $\sigma_{13}(\theta)$ for the temperature θ given in $(4.9)_1$, nucleation of the high-strain phase will occur at the left end of the bar; the critical elongation $\Delta_{13}(\theta)$ corresponding to $\sigma_{13}(\theta)$ is given by

$$\Delta_{13}(\theta) = \sigma_{13}(\theta)L/\mu\ . \tag{5.6}$$

As the phase boundary moves into the bar, the master equation (5.4) that controls its motion becomes a differential equation relating σ and Δ:

$$\frac{d\sigma}{d\Delta} = \frac{\mu}{L}\left[1 - \frac{\gamma_T}{q}\, v(\sigma, \theta)\right]; \tag{5.7}$$

here the kinetic response function v is understood to be given by (5.5). Thus the σ - Δ relation is the solution of the initial value problem consisting of (5.7) for $\Delta \geq 0$, together with the initial condition $\sigma = \sigma_{13}(\theta)$ at $\Delta = \Delta_{13}(\theta)$; this solution will depend on the temperature θ and the loading rate q as parameters.

One feature of the rate-dependent response governed by (5.7) may be noted immediately. The initial slope of the σ - Δ curve after nucleation will be negative for load rates q less than the critical value $\gamma_T\, v(\sigma_{13}(\theta), \theta)$, positive for load rates greater than this value . Thus depending on the loading rate, either "load drop" or "load rise" can occur in the initial response caused by the emergence of the phase boundary.

Suppose next that the constant-elongation-rate loading process is maintained until a value Δ_1 of the elongation is achieved; assume further that this occurs before the bar has transformed completely to the high-strain phase. At this instant, suppose that an unloading process is begun at the elongation rate - q, leading to a new initial value problem in which (5.7) is replaced by

$$\frac{d\sigma}{d\Delta} = \frac{\mu}{L}\left[1 + \frac{\gamma_T}{q}\, v(\sigma, \theta)\right], \tag{5.8}$$

for $\Delta \le \Delta_1$, together with the initial condition $\sigma = \sigma_1$ at $\Delta = \Delta_1$, where σ_1 is the final value of stress achieved according to (5.7) during loading. Unloading is presumed to continue until the stress is reduced to zero; as we shall see below, under some circumstances this occurs at a non-zero value of the elongation Δ, corresponding to permanent deformation of the bar. Phase boundary motion is the dissipative mechanism that permits this to occur, despite the fact that the material is thermoelastic.

In addition to the grip-controlled loading-unloading process described above, one can also consider isothermal *load*-controlled processes, in which one specifies a constant value of the stress rate $\dot{\sigma}$ (in addition to $\dot{\theta} = 0$) in the master equation (5.4).

Together, the respective solutions $\sigma = \sigma_L(\Delta)$ and $\sigma = \sigma_U(\Delta)$ to the grip-controlled loading and unloading initial value problems generate a hysteresis loop; this is illustrated schematically in Figure 7, which is drawn under the assumptions of load-rise and no permanent deformation. As indicated in the figure, this hysteresis loop must lie in the region described by $\sigma L/\mu \le \Delta \le (\gamma_T + \sigma/\mu)L$, $\sigma_m(\theta) \le \sigma \le \sigma_M(\theta)$, where θ is the temperature at which the experiment is conducted.

To investigate in detail the effect of temperature and load rate on the macroscopic response of the bar in isothermal grip-controlled stress cycles, we have undertaken some simple numerical computations. In carrying out these and later calculations, we make use of dimensionless phase boundary location s', time t', stress σ', temperature θ', elongation from the initial state Δ' and elongation rate q' defined as follows:

$$s' = s/L,\ t' = Rt/L\ ,\ \sigma' = \sigma/\mu\gamma_T\ ,\ \theta' = (\theta - \theta_0)/\theta_0,\ \Delta' = \Delta/L\gamma_T\ ,\ q' = q/R\gamma_T\ , \qquad (5.9)$$

where L is the referential length of the bar, R is the proportionality constant in the kinetic relation (5.5), μ is the elastic modulus of both phases, γ_T is the transformation strain and θ_0 is the transformation temperature. We also introduce dimensionless material parameters:

$$\left.\begin{aligned} &\alpha' = \alpha\theta_0/\gamma_T\ ,\ \theta'_* = (\theta_* - \theta_0)/\theta_0 > 0,\ M' = M\theta_0/\gamma_T\ ,\ m' = m\theta_0/\gamma_T\ , \\ &f'_{13} = f_{13}/\mu\gamma_T^2\ ,\ f'_{31} = f_{31}/\mu\gamma_T^2\ ,\ k' = rk\theta_0/(\mu\gamma_T^2)\ . \end{aligned}\right\} \qquad (5.10)$$

Except for the dimensionless nucleation parameters f'_{13} and f'_{31}, a single set of numerical values was assigned to these material parameters in the calulations underlying Figures 8 - 12 below: $\alpha' = 0.1$, $\theta'_* = 1$, $M' = 1.15$, $m' = 0.85$, $k' = 0.1$. (For this particular choice of material parameters, the latent heat λ_0 is indeed positive.) As regards the nucleation parameters, for Figures 9, 11 and 12, we take $f'_{13} = .28$, $f'_{31} = -.28$. In order to make clear the most significant features in Figure 10, the numerical values for the nucleation parameters have been chosen differently: we have taken $f'_{13} = 0.09$, $f'_{31} = -0.09$ in this case. Figure 8 does not depend on the nucleation parameters.

The nature of the kinetic response function V of (4.5) is illustrated in Figure 8, in which the dimensionless version $V' = V/R$ is plotted against the dimensionless driving traction

$f' = f/(\mu\gamma_T^2)$ at various dimensionless temperatures. According to the figure, increasing the temperature at a fixed level of driving traction *decreases* the velocity V of the moving interface. However, for the present model, the behavior of the interfacial velocity as a function of temperature at fixed driving traction is quite sensitive to the choice of material parameters. For example, if the value $m' = 0.85$ chosen above is replaced by $m' = 1.05$, then for an interval of temperature surrounding the transformation temperature, interfacial velocity is predicted to *increase* with increasing driving traction. In reporting experiments involving compression of single crystals of a particular CuAlNi alloy, Grujicic, Olson and Owen (1985b) show data in their Figure 5 indicating that interfacial velocity for slowly moving phase boundaries increases with temperature at each of several values of driving force.

Figure 9 shows the grip-controlled loading-unloading hysteresis loop for various dimensionless loading rates q' at a fixed dimensionless temperature θ'. The figure is based on direct numerical solution of the initial value problems for loading and unloading. At the lowest elongation rate (Figure 9(a)), the load drops after nucleation, whereas it rises at the higher load rates in Figures 9 (b)-(d). Figure 9(c) shows that permanent deformation can occur at higher load rates at this temperature. In Figures 9 (a)-(c), unloading was initiated before the bar transformed entirely to the high-strain phase. In contrast, Figure 9(d) describes the response when loading continues to the fully-transformed regime and beyond, followed by unloading that leads to nucleation of the *low-strain* phase at $x = L$ and to the eventual return of the bar to a stress-free state.

Figure 10 exhibits the grip-controlled macroscopic response of the bar predicted by the present model at various temperatures, all tests being carried out at the same elongation rate q' until the bar is completely transformed, with subsequent unloading at the rate $-q'$. The lowest value of dimensionless temperature represented in this figure is $\theta' = 0$, corresponding physically to a test carried out at the transformation temperature; permanent deformation occurs at this

temperature, as illustrated in Figure 10(a). Indeed, permanent deformation upon unloading to zero stress *must* occur at any temperature at or below the transformation temperature. This is because, when the latent heat λ_0 is positive, (3.27) shows that the Maxwell stress σ_0 is non-positive if $\theta' < 0$, and the entropy inequality prohibits leftward movement of the phase boundary at any stress level greater than σ_0. We note also that the principal effect of increasing temperature is to shift the hysteresis loop in the direction of increasing stress, without significantly altering the vertical "thickness" of the loop. In fact, the hysteresis loops in the four cases corresponding to positive temperature departures θ' are nearly congruent. Thus the hysteresis in these grip-controlled stress-elongation curves is essentially independent of temperature. This insensitivity of hysteresis to temperature is also predicted by the present model in isothermal *load-controlled* processes.

The shape of the calculated macroscopic response curves shown in Figures 9 and 10 is *qualitatively* similar to some - but not all - of those determined experimentally for a variety of alloys; see, for example, Grujicic, Olson and Owen (1985b), Krishnan and Brown (1973), Otsuka, Sakamoto and Shimizu (1979), Otsuka and Shimizu (1986), Pops (1970) and Müller and Xu (1991). In particular, substantial permanent deformation is found to occur at low temperatures but to be absent at high temperatures in experiments on AgCd (Krishnan and Brown, 1973) and NiTi (Otsuka and Shimizu, 1986), but some tests on CuZnSn indicate that permanent deformation may appear at higher temperatures, having been absent at lower ones (Pops, 1970). The prediction of the present model that the hysteresis loop is moved in the direction of increasing stress with little effect on the magnitude of the hysteresis itself seems to be consistent with experimental observations on CuZnSi (Pops, 1970), CuAlNi (Müller and Xu ,1991) and NiTi (Otsuka and Shimizu, 1986), but inconsistent with tests on CuZnSn (Pops, 1970). Experiments of Otsuka and Shimizu (1986) on CuAlNi seem to indicate that the magnitude of the hysteresis may increase or decrease with increasing temperature, depending on the type of martesite involved.

5.2. Thermal cycling at constant stress. We next consider a quasi-static process in which the stress is held constant while the temperature changes at a prescribed rate. Initially, the specimen is assumed to be at a given temperature greater than the transformation temperature θ_0 and under a stress σ. The bar is then cooled at a constant rate $\dot{\theta}$, the stress being maintained at the level σ. We seek to determine the relationship between the temperature θ and the elongation Δ relative to the initial configuration. During the initial period of cooling, the bar remains in the low-strain phase until the temperature has decreased to the nucleation value $\theta_{13}(\sigma)$ given by $(4.10)_1$ for the stress σ. Nucleation of the high-strain phase will then take place at the left end of the bar. After nucleation, a phase boundary will move into the specimen under the control of the master equation (5.4), which now becomes a differential equation relating the temperature θ and the elongation Δ during the cooling process, the stress and the cooling rate remaining as parameters. The Δ - θ relation during cooling is then determined as the solution of a suitable initial value problem.

The cooling process is continued until the bar has fully transformed to the high strain phase and beyond, terminating at some final temperature and a corresponding final elongation. The bar is then heated at a constant rate - $\dot{\theta}$ until the low-strain phase nucleates at x = L, the stress always remaining at the value σ. The master equation (5.4) and the appropriate nucleation condition lead to a new initial value problem whose solution relates Δ and θ during heating. The heating process is continued until the bar is fully transformed to the low-strain phase and beyond, with θ returning to its the initial value.

To illustrate the macroscopic response associated with the thermal cycling program described above, we have solved numerically the relevant initial value problems. In these computations, we have used the dimensionless variables and material constants introduced in (5.9) and (5.10). For the same numerical values of the material constants underlying Figure 9, we plot in Figure 11 the dimensionless temperature θ' versus the dimensionless elongation Δ' at

three values of the dimensionless stress σ', all curves corresponding to a common cooling/heating rate. The cooling process begins at the point A and terminates at B in each case; heating then returns the bar to the state corresponding to point A. The effect of increasing the level of stress is to move the hysteresis loop in the direction of increasing temperature without significantly increasing the thickness of the hysteresis loop itself.

The only thermal cycling experiments of which we are aware are those carried out by Burkart and Read (1953) on single crystals of indium-thallium at different levels of *compressive* stress. Because the stresses are compressive, the results of these experiments cannot be directly described by the present model. It may be noted, however, that the hysteresis loops reported in Figure 6 of the work of Burkart and Read correspond to thermal cycling at two different stresses. As in the predictions of the present model illustrated in Figure 11, these experimentally determined loops are moved in the direction of increasing temperature upon increase of the magnitude of the stress, and the amount of hysteresis seems not to be significantly different at the different stress levels.

5.3. The shape-memory effect. The shape-memory effect is exhibited under circumstances in which permanent deformation can occur during isothermal stress cycling. The specimen, which is initially in the low-strain phase at a given temperature and zero stress, is subjected to a four-stage program of thermomechanical loading. First, one stretches the bar at a constant elongation rate $\dot{\Delta}$ until it is fully transformed to the high-strain phase. In the second stage, unloading at the rate $-\dot{\Delta}$ is initiated and continued until the bar - still entirely in the high-strain phase - returns to a state with zero stress but non-zero elongation, corresponding to permanent deformation. Throughout the stress cycle, the temperature has remained at its intial value. In stage three, the stress is kept at the value zero while the specimen is heated at a constant rate $\dot{\theta}$ until nucleation of the low-strain phase occurs. Heating continues until the bar has fully transformed to the low-strain phase, still at zero stress but at some non-zero value of

elongation and at a high temperature. In the fourth and final stage, stress-free cooling is used to restore the bar to its initial length and temperature.

To illustrate the shape-memory effect as manifested by the present thermoelastic model, we have numerically integrated the master equation (5.4) in a program of mechanical and thermal loading and unloading of the kind described above. The initial temperature is taken to be the transformation temperature ($\theta' = 0$). The corresponding stress-elongation and temperature-elongation relations are shown in Figure 12, based on calculations that utilize the same values of the dimensionless material parameters underlying Figure 9. Note that dimensionless stress is plotted on the upper half of the vertical axis, dimensionless temperature on the lower half; the horizontal axis represents dimensionless elongation relative to the initial state. Stage one corresponds to mechanical loading along OAB of the stress-elongation curve. Stage two consists of unloading from B to a permanently deformed state C. In stage three, the bar is heated until it is fully transformed to the low strain phase (CDE in the figure). Finaly, cooling takes place along EO until the specimen has returned to its initial state. Figure 12 is qualitatively similar to the schematic description of the shape-memory effect given by Krishnan, Delaey, Tas and Warlimont (1974) in their Figure 11.

References

Abeyaratne, R. and Knowles, J.K., 1988, On the dissipative response due to discontinuous strains in bars of unstable elastic material, *International Journal of Solids and Structures*, **24**, pp. 1021-1042.

Abeyaratne, R. and Knowles, J.K., 1990, On the driving traction acting on a surface of strain discontinuity in a continuum, *Journal of the Mechanics and Physics of Solids*, **38**, pp. 345-360.

Abeyaratne, R. and Knowles, J.K., 1991a , Kinetic relations and the propagation of phase boundaries in solids, *Archive for Rational Mechanics and Analysis*, **114**, pp. 119-154.

Abeyaratne, R. and Knowles, J.K., 1991b, Implications of viscosity and strain gradient effects for the kinetics of propagating phase boundaries in solids, *SIAM Journal on Applied Mathematics*, **51**, pp. 1205-1221.

Abeyaratne, R. and Knowles, J.K., 1992a, On the propagation of maximally dissipative phase boundaries in solids, *Quarterly of Applied Mathematics*, **50**, pp. 149-172.

Abeyaratne, R. and Knowles, J.K., 1992b, Nucleation, kinetics and admissibility criteria for propagating phase boundaries, to appear in *Proceedings of the Workshop on Shock Induced Transitions and Phase Structures in General Media*, (E. Dunn, R. Fosdick and M. Slemrod, eds.), Institute of Mathematics and its Applications, University of Minnesota.

Achenbach, M. and Müller, I. , 1985, Simulation of material behavior of alloys with shape memory, *Archives of Mechanics*, **37**, pp. 573-585.

Burkart, M.W. and Read, T.A., 1953, Diffusionless phase change in the indium-thallium system, *Journal of Metals, Transactions of the AIME*, **197**, pp. 1516-1524.

Ericksen, J.L., 1975, Equilibrium of bars, *Journal of Elasticity*, **5**, pp. 191-201.

Falk, F. 1980, Model free energy, mechanics and thermodynamics of shape-memory alloys, *Acta Metallurgica*, **28**, pp. 1773-1780.

Falk, F., 1988, On the motion of martensitic domain walls in shape-memory alloys, in *Phase transformations*, (G.W. Lorimer, ed.), Inst of Metals, London, pp. 77-79.

Grujicic, M., Olson, G.B. and Owen, W.S., 1985a, Mobility of martensite interfaces, *Metallurgical Transactions*, **16A**, pp. 1713-1722.

Grujicic, M., Olson, G.B. and Owen, W.S., 1985b, Mobility of the β_1-γ_1' martensitic interface in CuAlNi: Part I. Experimental measurements, *Metallurgical Transactions*, **16A** , pp. 1723-1734.

Jiang, Q., 1988, A continuum model for phase transformation in thermoelastic solids, Technical Report No. 9, U.S. Office of Naval Resear Contract N00014-87-K-0117, California Institute of Technology, to appear in *Journal of Elasticity*.

Knowles, J.K., 1979, On the dissipation associated with equilibrium shocks in finite elasticity, *Journal of Elasticity*, **9**, pp. 131-158.

Krishnan, R.V. and Brown, L.C., 1973, Pseudo-elasticity and the strain-memory effect in an Ag-45 at. pct. Cd alloy, *Metallurgical Transactions*, **4**, pp. 423-429.

Krishnan, R.V., Delaey, L., Tas, H. and Warlimont, H., 1974, Thermoplasticity, pseudoelasticity and the memory effects associated with martensitic transformations. Part 2. The macroscopic mechanical behavior, *Journal of Materials Science*, **9**, pp. 1536-1544.

Müller, I. and Wilmansky, K., 1981, Memory alloys - phenomenology and Ersatzmodel, in *Continuum Models of Discrete Systems*, (O. Brulin and R.K.T. Hsieh, eds.), North Holland, Amsterdam, pp. 495-509.

Müller, I. and Xu, H. , 1991, On the pseudo-elastic hysteresis, *Acta Metallurgica et Materialia*, **39**, pp. 263-271.

Otsuka, K., Sakamoto, H. and Shimizu, K., 1979, Succesive stress-induced martensitic transformations and associated transformation pseudo-elasticity in Cu-Al-Ni alloys, *Acta Metallurgica*, **27**, pp. 585-601.

Otsuka, K. and Shimizu, K., 1986, Pseudo-elasticity and shape-memory effects in alloys, *International Metals Reviews*, **31**, pp. 93-114.

Pippard, A.B., 1985, *Response and Stability*, Cambridge University Press, Cambridge.

Pops, H., 1970, Stress-induced pseudo-elasticity in ternary Cu-Zn based beta prime phase alloys, *Metallurgical Transactions*, **1**, pp. 251-258.

Porter, D.A. and Easterling, K.E., 1981, *Phase Transformations in Metals and Alloys*, van Nostrand-Reinhold, New York.

Tanaka, K., Tobushi, H. and Iwanaga, H., 1988, Continuum mechanical approach to thermomechanical behavior of TiNi alloys, in *Proceedings of the 31st Japan Congress on Materials Research*, (K. Komai, ed.), Society of Materials Science, Kyoto, pp. 51-56.

Weiner, J. 1970, Thermal activation and tunneling phenomena in solids, *Proceedings of the Sixth U.S. National Congress of Applied Mechanics*, (G. Carrier, ed.), ASME Publishers, New York, pp. 62-77.

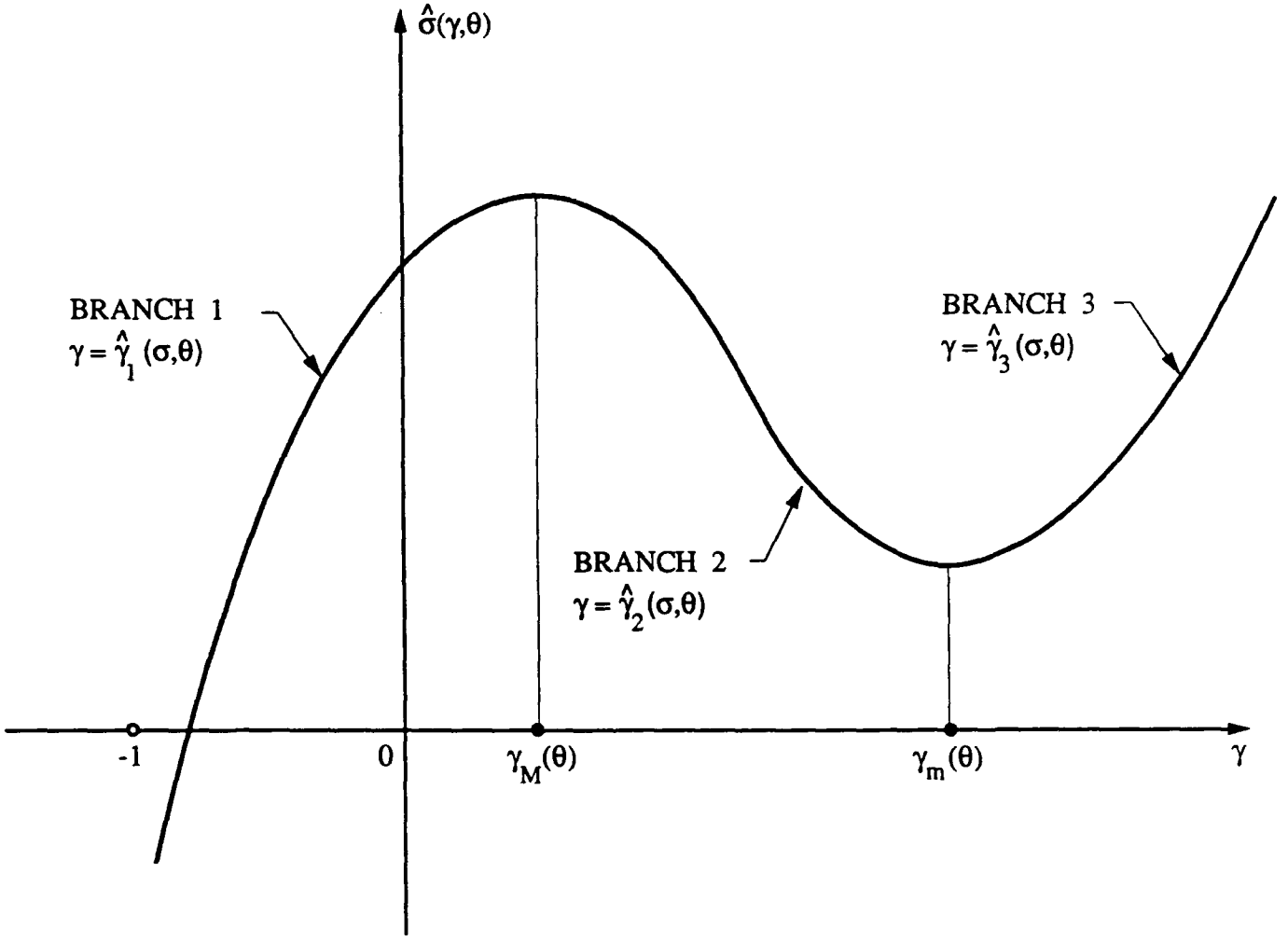

FIGURE 1. STRESS-STRAIN CURVE $\sigma = \hat{\sigma}(\gamma,\theta)$ AT A FIXED TEMPERATURE θ.

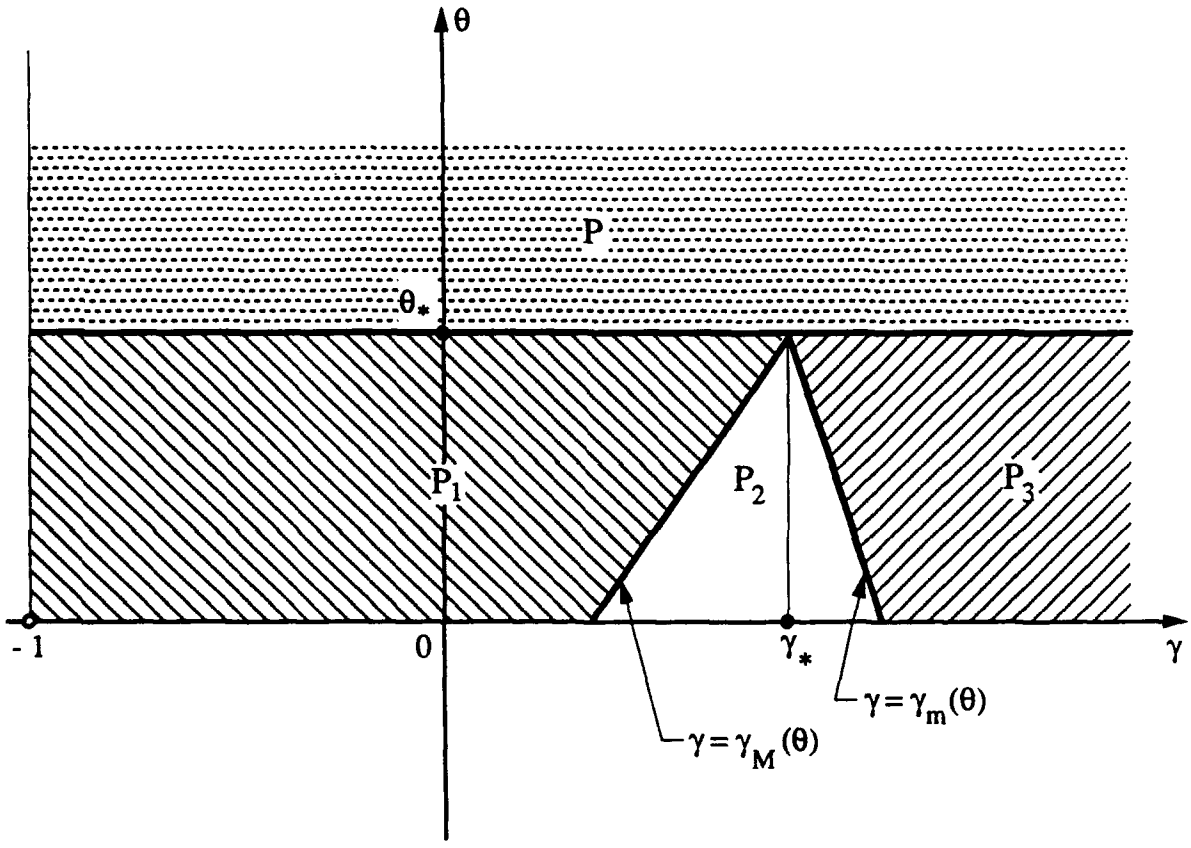

FIGURE 2. REGIONS P, P_1, P_2 AND P_3 IN THE STRAIN-TEMPERATURE PLANE ; SEE (3.3) - (3.5) .

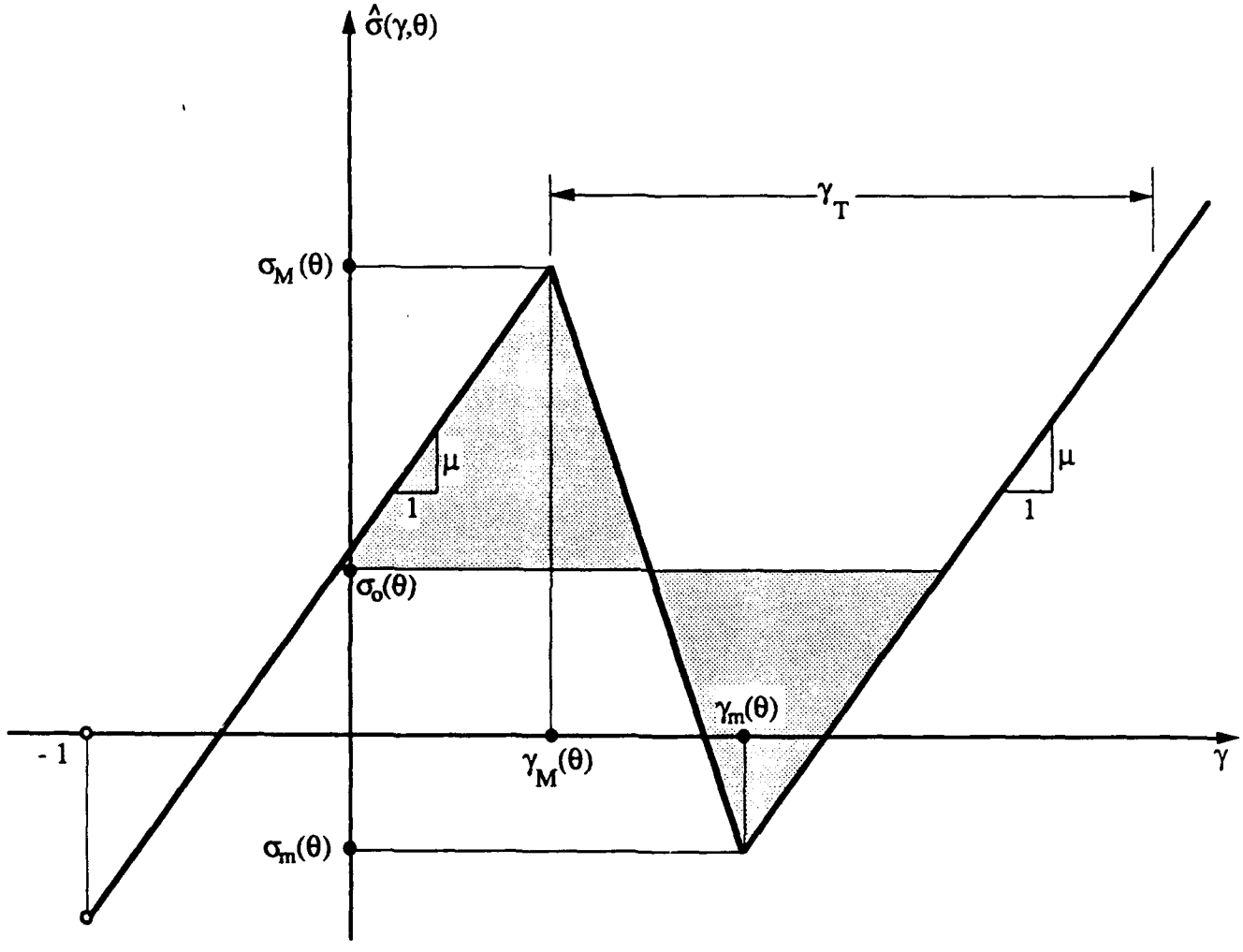

FIGURE 3. THE TRILINEAR STRESS-STRAIN CURVE AT A FIXED TEMPERATURE θ.

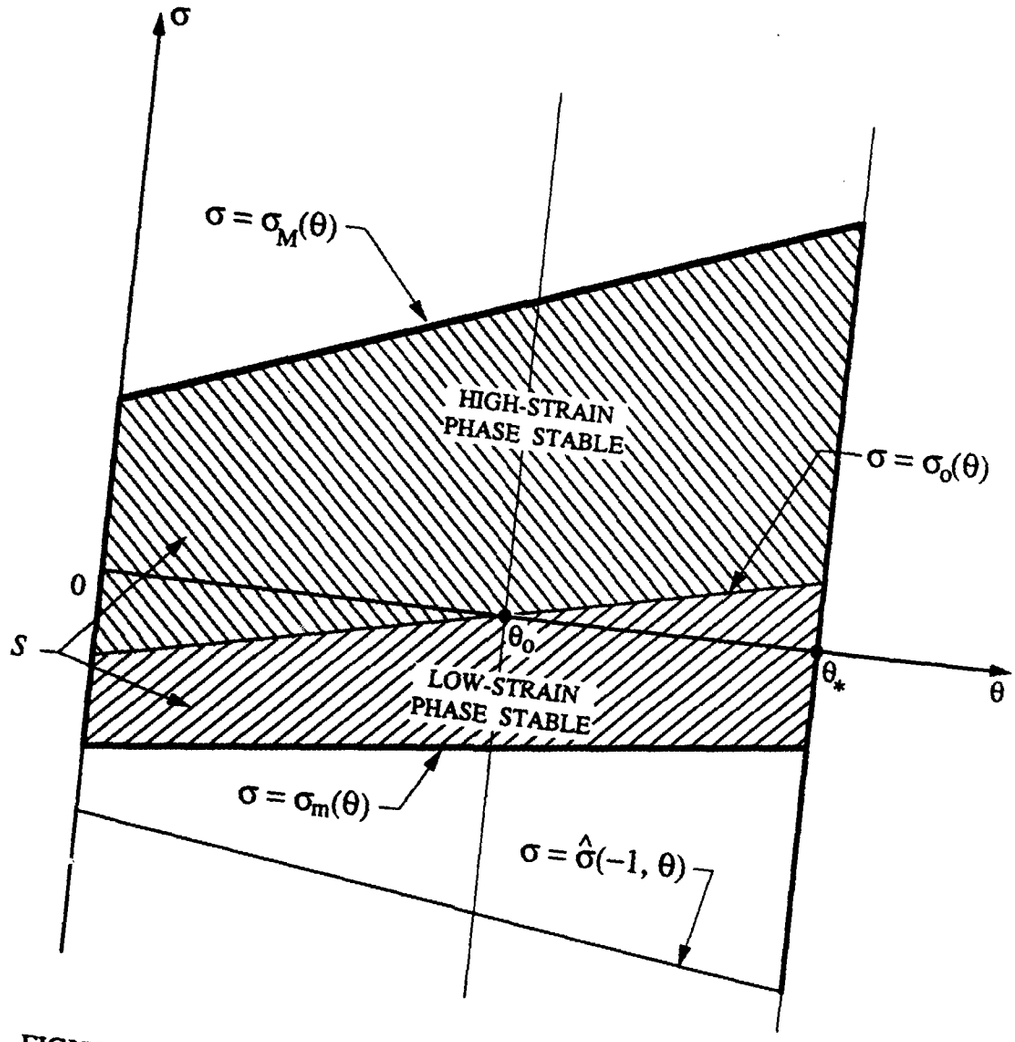

FIGURE 4. REGION S OF COEXISTENCE OF LOW- AND HIGH-STRAIN PHASES IN THE TEMPERATURE - STRESS PLANE.

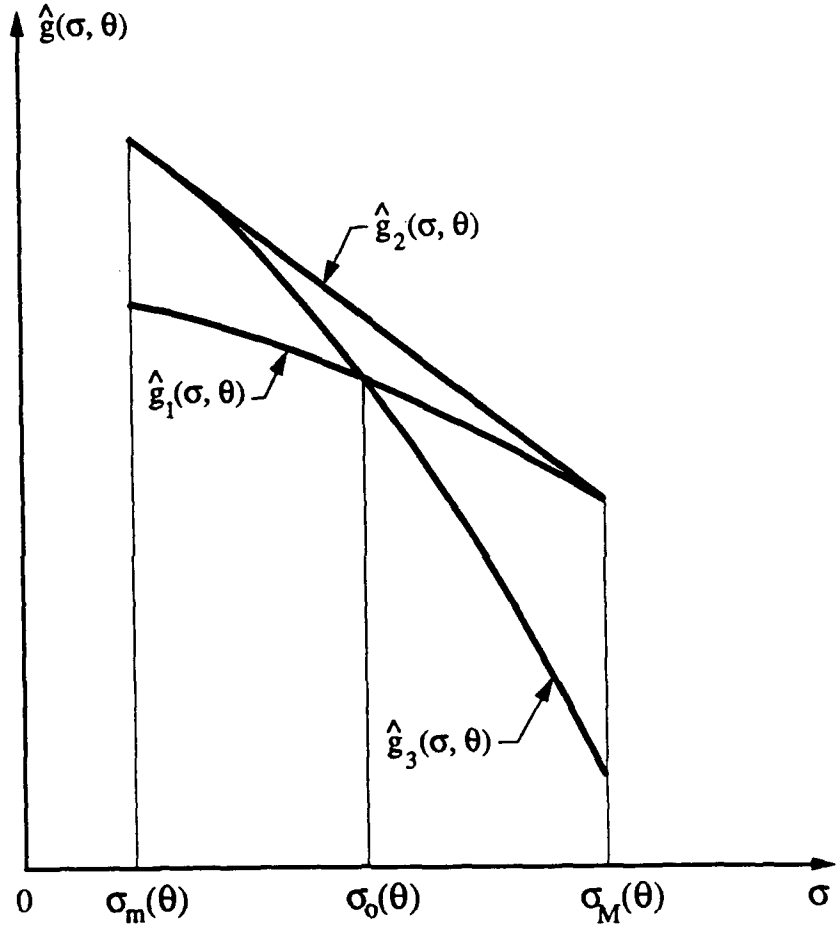

FIGURE 5. GIBBS FREE ENERGIES FOR THE VARIOUS PHASES AS FUNCTIONS OF STRESS AT A FIXED TEMPERATURE $\theta > \theta_o$.

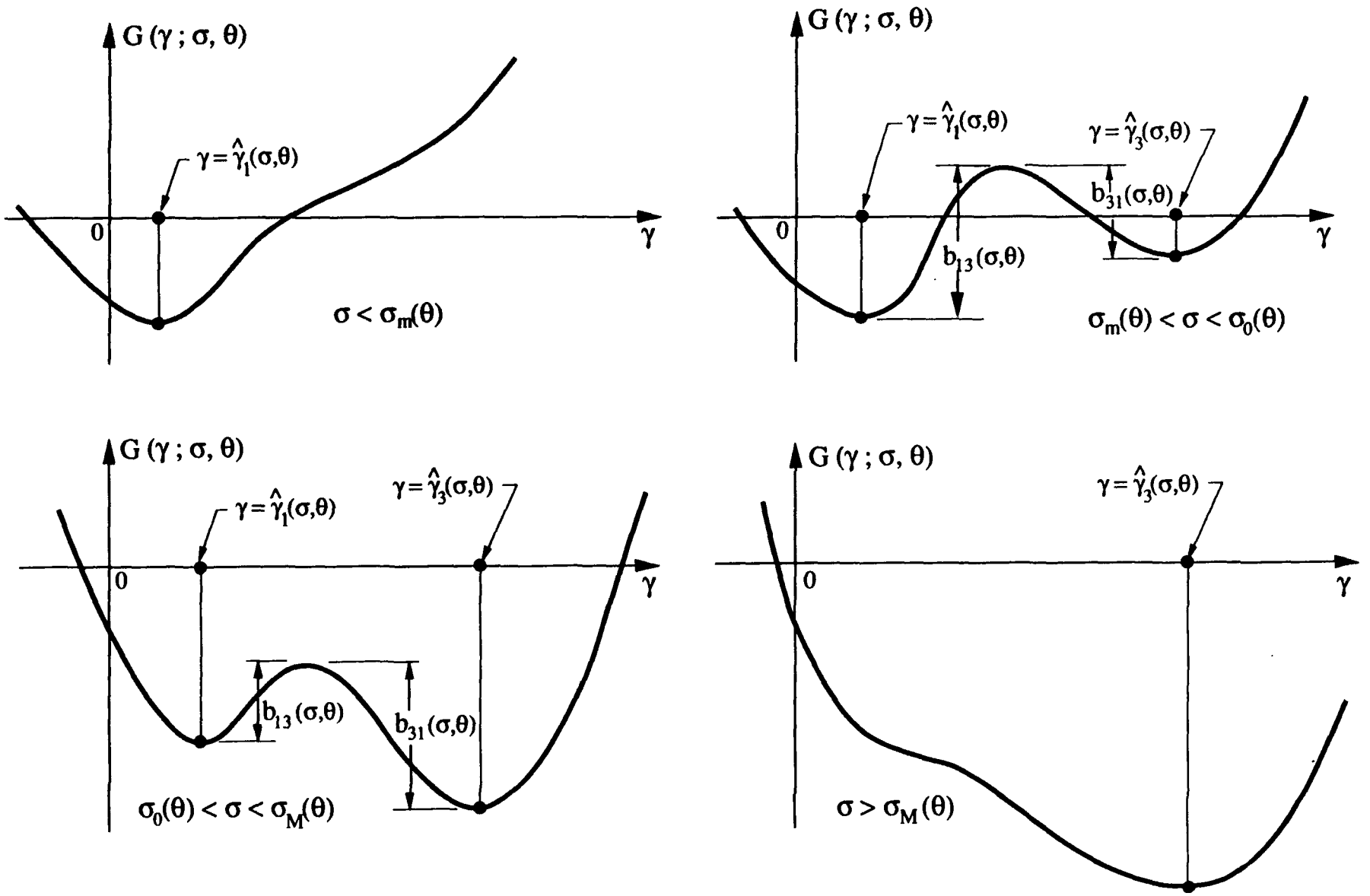

FIGURE 6. THE POTENTIAL $G(\gamma; \sigma, \theta)$ AS A FUNCTION OF γ FOR VARIOUS VALUES OF σ ; θ IS FIXED.

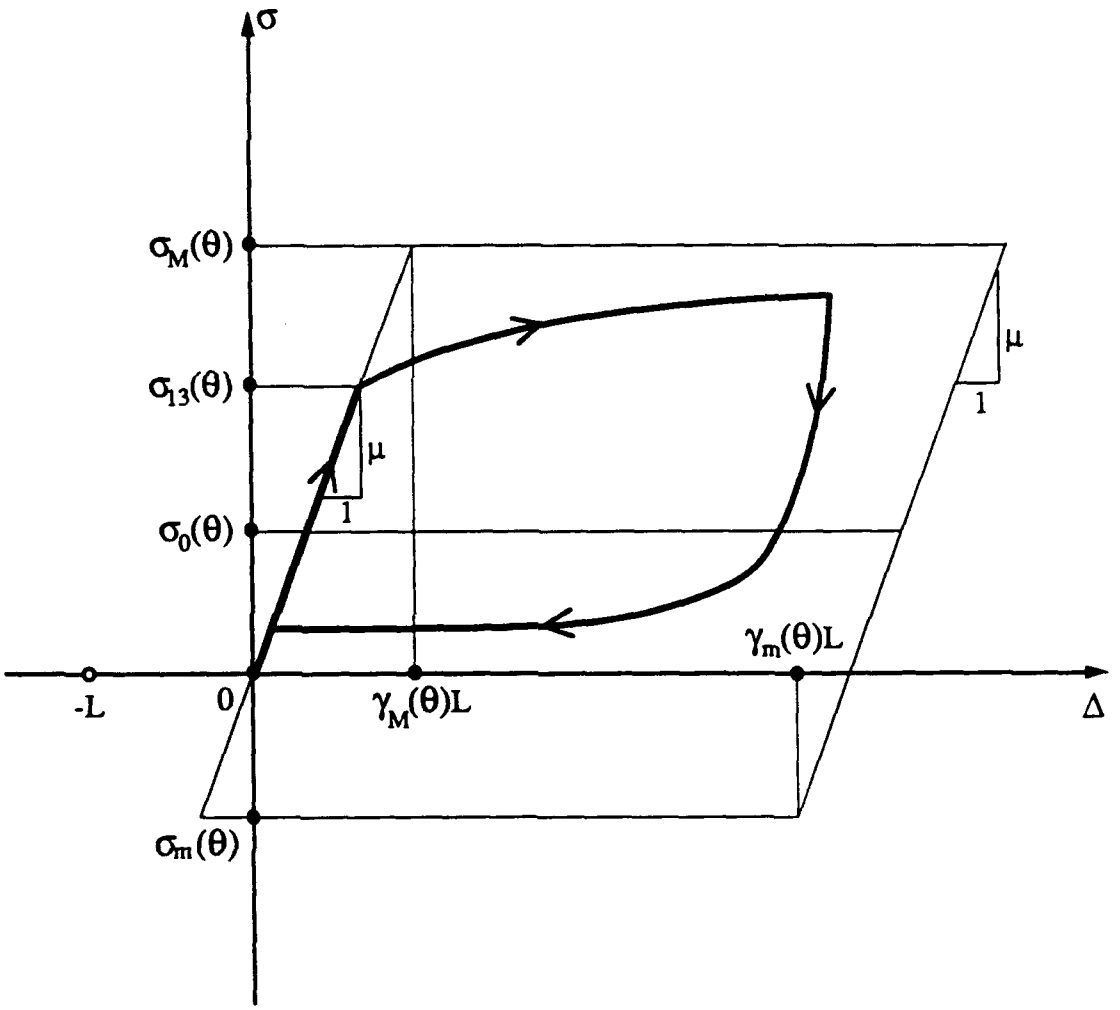

FIGURE 7. SCHEMATIC MECHANICAL LOADING-UNLOADING HYSTERESIS LOOP AT CONSTANT TEMPERATURE.

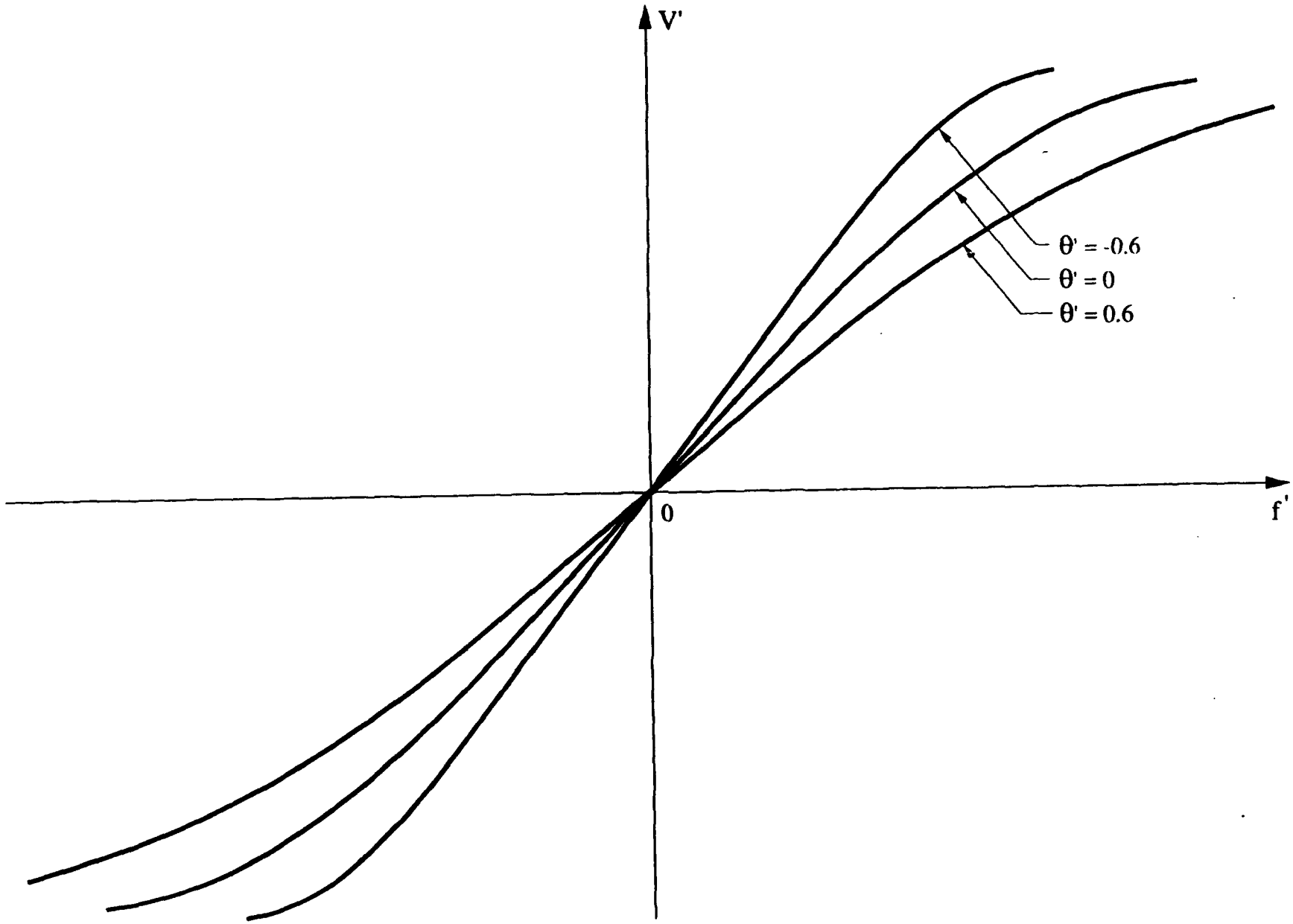

FIGURE 8. PHASE BOUNDARY VELOCITY AS A FUNCTION OF DRIVING TRACTION AT VARIOUS TEMPERATURES.

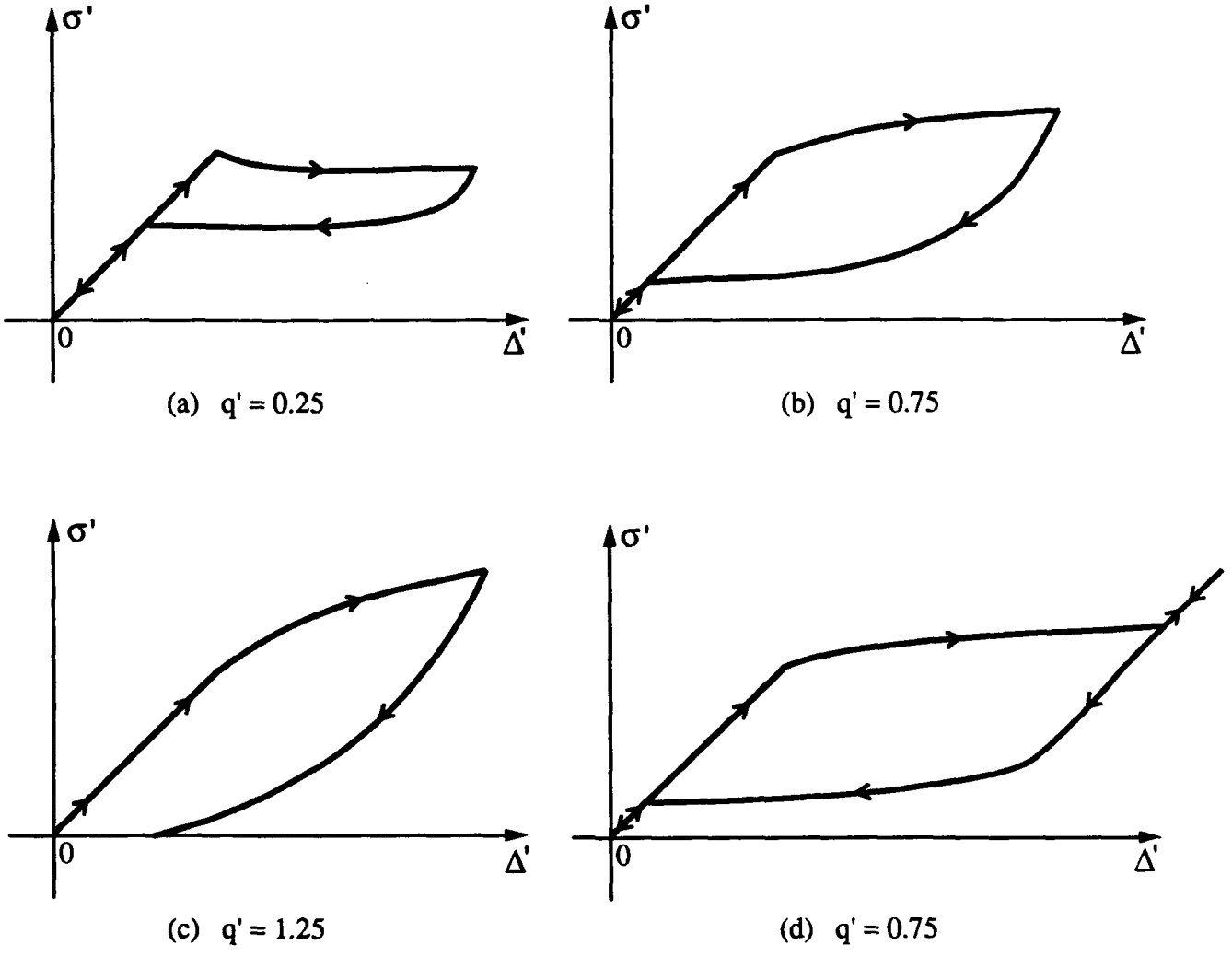

(a) $q' = 0.25$

(b) $q' = 0.75$

(c) $q' = 1.25$

(d) $q' = 0.75$

FIGURE 9. MECHANICAL CYCLING AT VARIOUS ELONGATION RATES q', ALL AT THE SAME TEMPERATURE $\theta' = 0.4$.

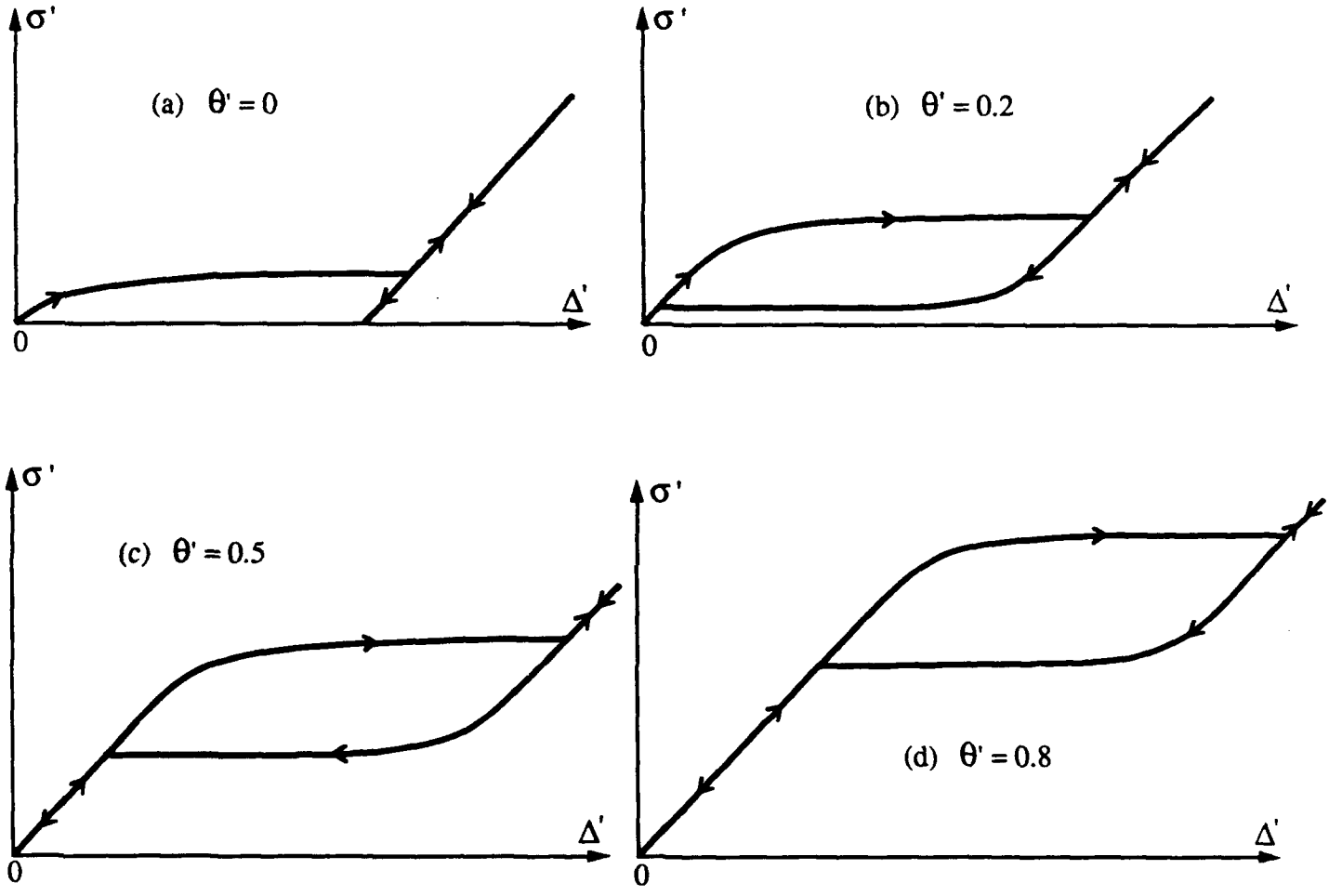

FIGURE 10. MECHANICAL CYCLING AT VARIOUS TEMPERATURES, ALL AT THE SAME ELONGATION RATE q' = 0.5.

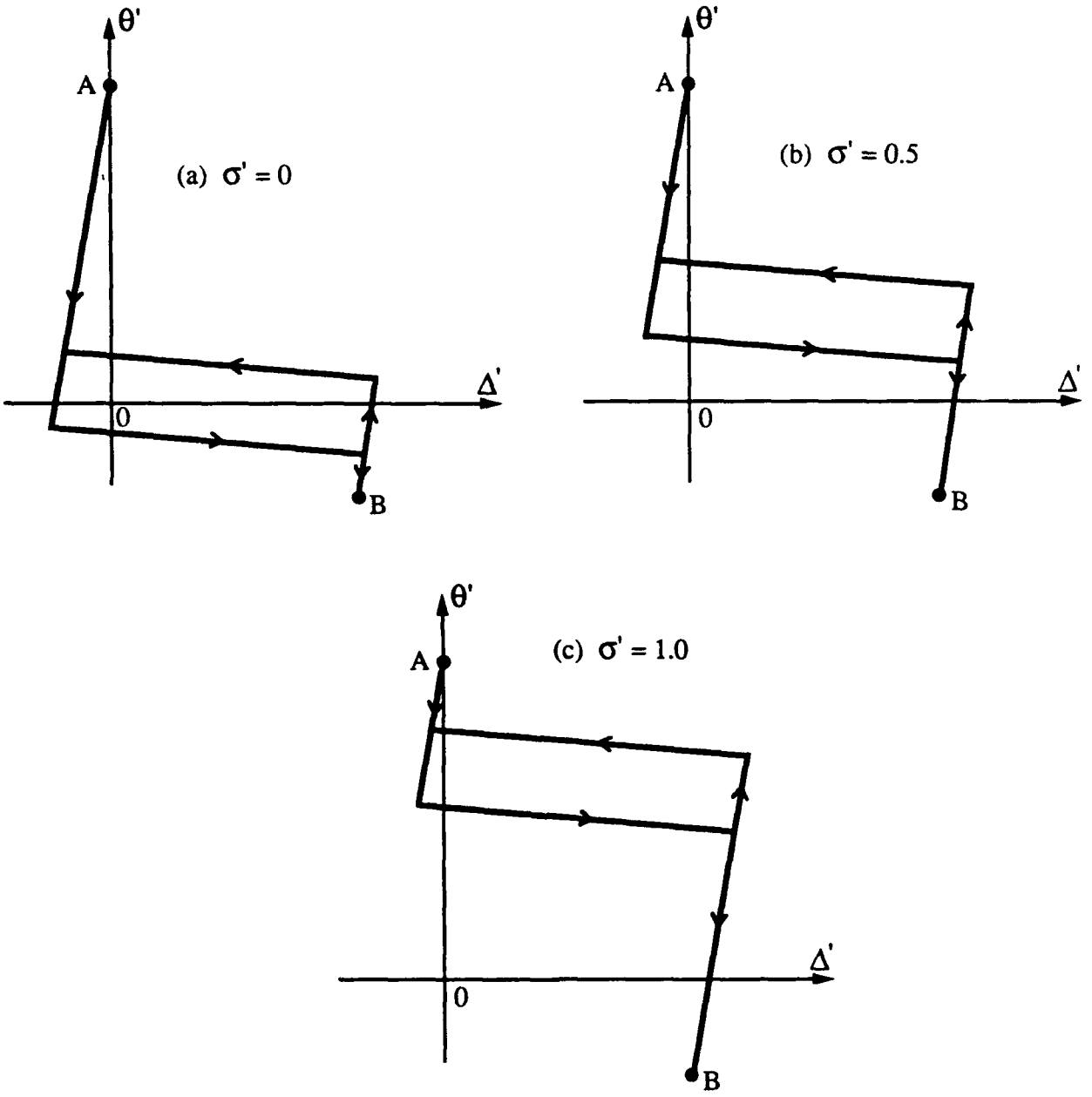

FIGURE 11. THERMAL CYCLING AT VARIOUS STRESSES, ALL AT THE SAME COOLING RATE $\dot{\theta}' = -0.1$.

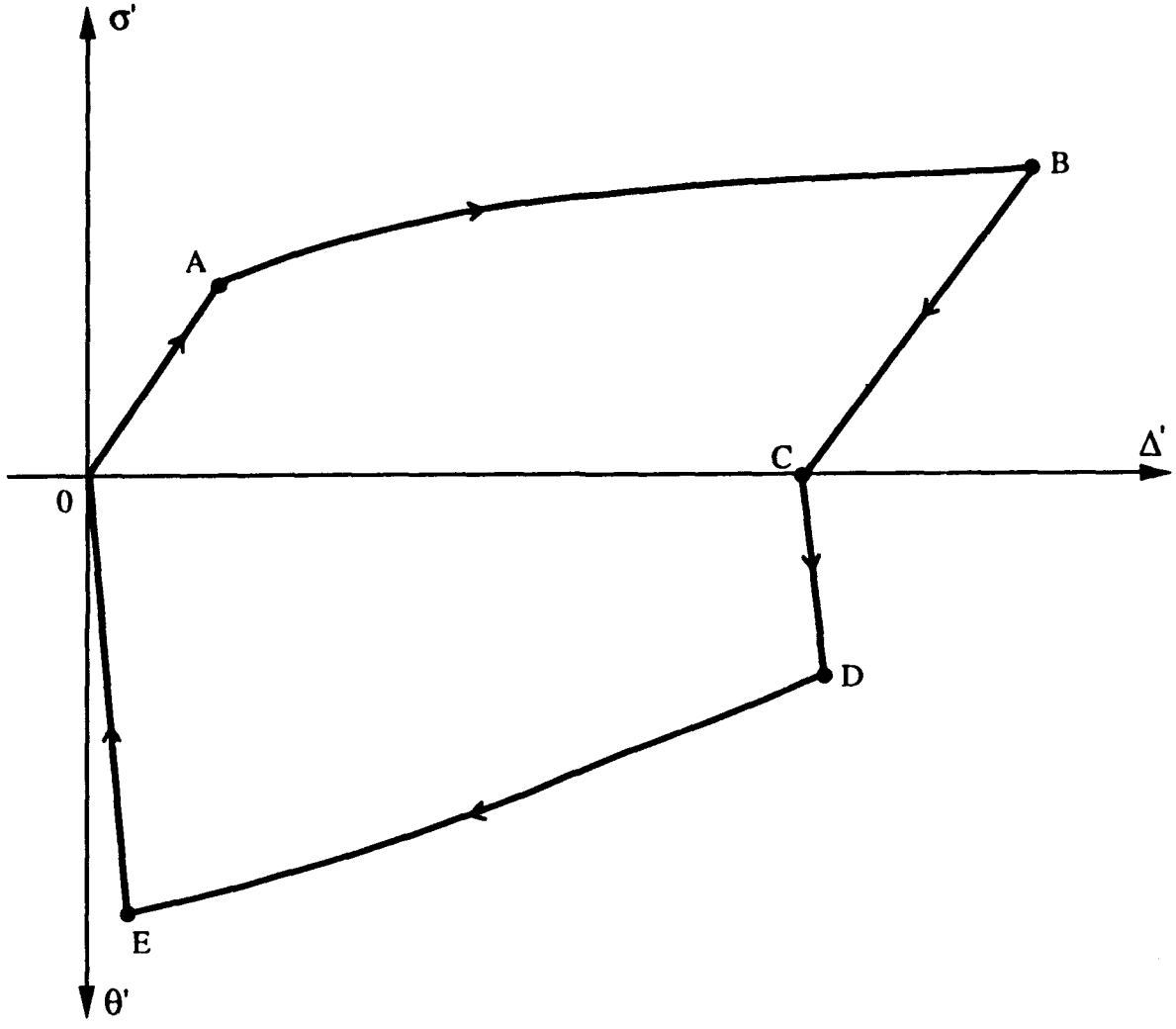

FIGURE 12. THE SHAPE-MEMORY EFFECT: INITIAL TEMPERATURE $\theta' = 0$, FIRST STAGE ELONGATION RATE $q' = 1.0$, THIRD STAGE HEATING RATE $\dot{\theta}' = 0.2$.

REPORT DOCUMENTATION PAGE

Form Approved
OMB No. 0704-0188

1a. REPORT SECURITY CLASSIFICATION Unclassified	1b. RESTRICTIVE MARKINGS
2a. SECURITY CLASSIFICATION AUTHORITY	3. DISTRIBUTION/AVAILABILITY OF REPORT Unlimited
2b. DECLASSIFICATION/DOWNGRADING SCHEDULE	
4. PERFORMING ORGANIZATION REPORT NUMBER(S) Technical Report No. 7	5. MONITORING ORGANIZATION REPORT NUMBER(S)
6a. NAME OF PERFORMING ORGANIZATION Calif. Institute of Technology 6b. OFFICE SYMBOL (If applicable)	7a. NAME OF MONITORING ORGANIZATION Office of Naval Research
6c. ADDRESS (City, State, and ZIP Code) Pasadena, CA 91125	7b. ADDRESS (City, State, and ZIP Code) 565 S. Wilson Ave. Pasadena, CA 91106
8a. NAME OF FUNDING/SPONSORING ORGANIZATION Office of Naval Research 8b. OFFICE SYMBOL (If applicable)	9. PROCUREMENT INSTRUMENT IDENTIFICATION NUMBER
8c. ADDRESS (City, State, and ZIP Code) 800 N. Quincy St. Arlington, VA 22217	10. SOURCE OF FUNDING NUMBERS PROGRAM ELEMENT NO. / PROJECT NO. / TASK NO / WORK UNIT ACCESSION NO

11. TITLE (Include Security Classification)
A Continuum Model of a Thermoelastic Solid Capable of Undergoing Phase Transitions

12. PERSONAL AUTHOR(S)
R. Abeyaratne and J. K. Knowles

13a. TYPE OF REPORT	13b. TIME COVERED	14. DATE OF REPORT (Year, Month, Day)	15. PAGE COUNT
Technical	FROM _____ TO _____	April, 1992	55

16. SUPPLEMENTARY NOTATION

17. COSATI CODES			18. SUBJECT TERMS (Continue on reverse if necessary and identify by block number)
FIELD	GROUP	SUB-GROUP	

19. ABSTRACT (Continue on reverse if necessary and identify by block number)

We construct explicitly a Helmholtz free energy, a kinetic relation and a nucleation criterion for a one-dimensional thermoelastic solid capable of undergoing either mechanically- or thermally-induced phase transitions. We study the hysteretic macroscopic response predicted by this model in the case of quasi-static processes involving stress cycling at constant temperature, thermal cycling at constant stress, or a combination of mechanical and thermal loading that gives rise to the shape-memory effect. These predictions are compared qualitatively with experimental results.

20. DISTRIBUTION/AVAILABILITY OF ABSTRACT ☒ UNCLASSIFIED/UNLIMITED ☐ SAME AS RPT ☐ DTIC USERS	21. ABSTRACT SECURITY CLASSIFICATION Unclassified
22a. NAME OF RESPONSIBLE INDIVIDUAL James K. Knowles	22b. TELEPHONE (Include Area Code) 818-356-4135 22c. OFFICE SYMBOL